nanomaterials

MDPI

Review

Properties and Characterization Techniques of Graphene Modified Asphalt Binders

Rodrigo Polo-Mendoza [1], Tatiana Navarro-Donado [2], Daniela Ortega-Martinez [2,3], Emilio Turbay [2], Gilberto Martinez-Arguelles [2,*] and Rita Peñabaena-Niebles [4]

[1] Faculty of Science, Charles University, 128 00 Prague, Czech Republic
[2] Department of Civil & Environmental Engineering, Universidad del Norte, Barranquilla 081001, Colombia
[3] School of Civil and Environmental Engineering, Technische Universität Dresden, 01069 Dresden, Germany
[4] Department of Industrial Engineering, Universidad del Norte, Barranquilla 081001, Colombia
* Correspondence: garguelles@uninorte.edu.co

Abstract: Graphene is a carbon-based nanomaterial used in various industries to improve the performance of hundreds of materials. For instance, graphene-like materials have been employed as asphalt binder modifying agents in pavement engineering. In the literature, it has been reported that (in comparison to an unmodified binder) the Graphene Modified Asphalt Binders (GMABs) exhibit an enhanced performance grade, a lower thermal susceptibility, a higher fatigue life, and a decreased accumulation of permanent deformations. Nonetheless, although GMABs stand out significantly from traditional alternatives, there is still no consensus on their behavior regarding chemical, rheological, microstructural, morphological, thermogravimetric, and surface topography properties. Therefore, this research conducted a literature review on the properties and advanced characterization techniques of GMABs. Thus, the laboratory protocols covered by this manuscript are atomic force microscopy, differential scanning calorimetry, dynamic shear rheometer, elemental analysis, Fourier transform infrared spectroscopy, Raman spectroscopy, scanning electron microscopy, thermogravimetric analysis, X-ray diffraction, and X-ray photoelectron spectroscopy. Consequently, the main contribution of this investigation to the state-of-the-art is the identification of the prominent trends and gaps in the current state of knowledge.

Keywords: asphalt binder; graphene; graphene-like materials; modifying agents; nanomaterials

Citation: Polo-Mendoza, R.; Navarro-Donado, T.; Ortega-Martinez, D.; Turbay, E.; Martinez-Arguelles, G.; Peñabaena-Niebles, R. Properties and Characterization Techniques of Graphene Modified Asphalt Binders. *Nanomaterials* **2023**, *13*, 955. https://doi.org/10.3390/nano13050955

Academic Editor: Alexander Lukin

Received: 5 February 2023
Revised: 20 February 2023
Accepted: 22 February 2023
Published: 6 March 2023

1. Introduction

Transportation infrastructure is a crucial element for the socioeconomic development of communities [1–4]. The preceding is evident in the growth of pavement construction and maintenance projects worldwide [5–8]. Notably, most of the road infrastructure in the world corresponds to asphalt pavements [4,9,10]. In this way, the demand for asphalt binders has soared at an accelerated rate. Consequently, the environmental impacts of this industry are immense and tend to grow over the years [11–13]. Therefore, researchers have proposed various strategies to decrease these environmental burdens [14–16]. One of the most promising alternatives is the production of high-performance asphalt binders [17–19]. The concept behind this approach states that employing materials with a longer useful life can mitigate the depletion of raw materials (i.e., non-renewable resources) and, thus, increase sustainability (both in environmental and economic criteria) in the long term [20–22].

Overall, high-performance asphalt binders are achieved by mixing the virgin/pristine binder with an additive agent [23–26]. Within these materials, the Graphene Modified Asphalt Binders (GMABs) stand out for their excellent mechanical behavior in a wide range of temperatures and frequencies [27–30]. The GMABs are the result of modifying the asphalt binder with graphene-like materials (i.e., graphene and its derivatives) [31–34]. Although there are many derivatives of graphene, only two are widely used in pavement engineering:

Graphene Oxide (GO) and Graphene Nanoplatelets (GNPs) [35–38]. Remarkably, the flake graphite and expanded graphite nanosheets are other derivatives utilized to improve the engineering characteristics of asphalt binders [31,32,39].

In the last two decades, nanomaterials have been used with great notoriety to modify a broad type of materials, including asphalt binders [18,40–42]. The main nanomaterials employed for developing high-performance asphalt binders are chemical compounds based on carbon, for instance, graphene-like materials, carbon nanotubes, and nanoclays [43,44]. These modified asphalt binders are attractive because they (adequately) support high-traffic loads under harsh external conditions (i.e., high humidity, great environmental salinity, and intense ultraviolet radiation) at high and low temperatures [10,35,45]. Notably, the GMABs are one of the most versatile and resistant binders (i.e., provide an augmented service life) since they simultaneously improve fatigue and rutting resistances [31,32,36,46]. The preceding is particularly important because the asphalt mixtures (and successively the asphalt pavement structures) tend to fail mainly due to distresses associated with low fatigue life and raised accumulation of permanent deformations [18,38,40,47]. Another of the primary advantages of GMABs is that they are favorably compatible (to be blended) with other technologies, such as crumb rubber, electric arc furnace slag, epoxy resins, polystyrene, and Styrene-Butadiene-Styrene (SBS) [38,48–52].

Unlike neat asphalt binders, GMABs have such a complex chemical structure that they cannot be characterized only with traditional laboratory tests (i.e., density, penetration, softening point, dynamic viscosity, ductility, flash point, and solubility) [4,21,32,46,49]. Thus, in order to adequately describe the GMABs, it is necessary to carry out evaluations of their chemical, rheological, microstructural, morphological, thermogravimetric, and surface topography properties [34,53–55]. However, there is still no consensus in the literature on what particular tests should be conducted for these characterizations; moreover, there is much less consensus on the behavior of the GMABs under these laboratory protocols [31,32].

The preceding situation has motivated this manuscript to develop a comprehensive literature review on the properties and characterization techniques of GMABs. In this way, the main objective of this manuscript is to identify the main trends and gaps in the current state-of-the-art. Thus, it is expected that this investigation encourages researchers to improve their current practices and address those aspects that are still susceptible to improvement in the future. It is important to note that the scope of this review is limited to three graphene-like materials, i.e., graphene, GO, and GNPs.

Following, the structure of the subsequent sections of this paper is described. Section 2 presents the basics of the asphalt binder, emphasizing the aspects related to its chemistry. Next, Section 3 clarifies the essential concepts and features of graphene-like materials. In Section 4, the properties of GMABs are detailed together with the main modification processes. Likewise, Section 5 examines the state-of-the-art characterization techniques for GMABs, i.e., Atomic Force Microscopy (AFM), Differential Scanning Calorimetry (DSC), Dynamic Shear Rheometer (DSR), Elemental Analysis (EA), Fourier Transform Infrared Spectroscopy (FTIR), Raman Spectroscopy (RS), Scanning Electron Microscopy (SEM), Thermogravimetric Analysis (TGA), X-ray Diffraction (XRD), and X-ray Photoelectron Spectroscopy (XPS). Successively, in Section 6, there is a discussion about the trends and gaps in the literature. Then, Section 7 proposes recommendations for future research lines. Finally, Section 8 lists the main conclusions of this investigation.

2. Basics of Asphalt Binder

Asphalt binder is one of the derivatives obtained from refining crude oil (also named petroleum) [56–62]. Asphalt binder is a material with outstanding hydrophobicity and excellent adhesion capabilities, allowing it to be employed in a wide range of applications, for instance, as a binder for producing composite materials (e.g., asphalt mastic and asphalt mixtures) and as a coating membrane for waterproofing projects [9,63–68].

Due to the variety of petroleum sources, each asphalt binder has a distinct chemical composition and a distinct performance for engineering applications [59,69]. Beyond these differences, asphalt binders can be chemically described as an intricate combination of thousands of hydrocarbon molecules, oxygen compounds, and small amounts of nitrogen and sulfur compounds with traces of metals [57,70–76]. Notably, a singular assortment of hydrocarbon and oxygen compounds generates a specific temperature-dependent viscoelastic behavior [67,77]. These compounds can be classified from lower to higher polarity as Saturates, Aromatics, Resins, and Asphaltenes, i.e., the so-called SARA fractions [74,78–80]. Figure 1 illustrates their standard molecular structure. Remarkably, the SARA fractions are a colloidal system in which micelles of asphaltenes remain in maltenes (i.e., aromatics, resins, and asphaltenes) [63,73]. In other words, the high polar solid particles are dispersed constantly in the low polar oily environment [81–83]. Figure 2 exhibits a sketch of this model.

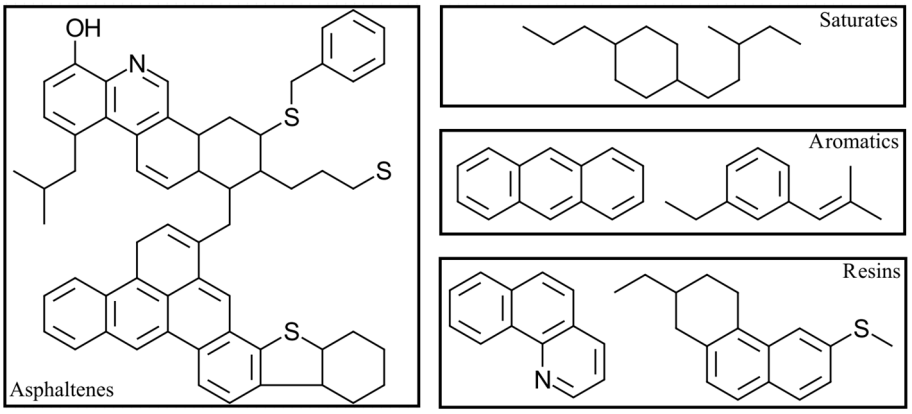

Figure 1. Standard molecular structure of the SARA fractions. Adapted from [3].

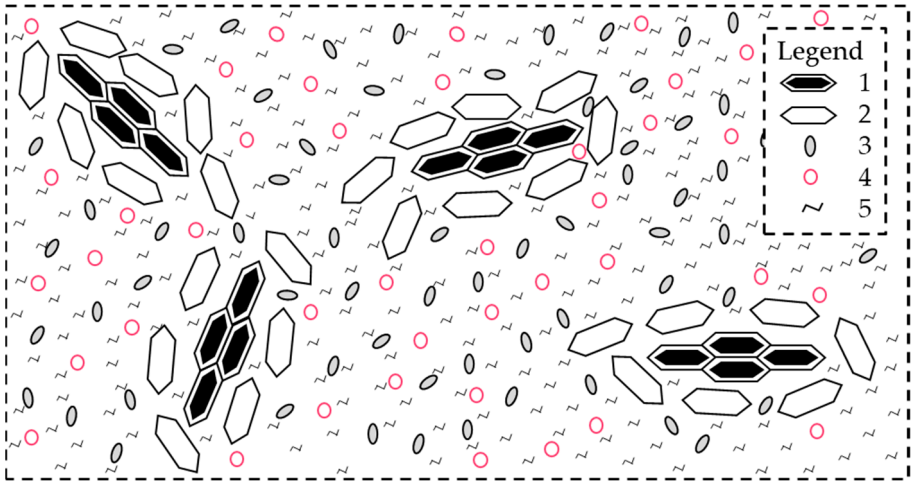

Figure 2. Colloidal model of the asphalt binder. Adapted from [3]. Legend: 1—central part of the asphaltene; 2—compounds with aromatic nature and high molecular weight; 3—compounds with prevalent aromatic nature and low molecular weight; 4—compounds of mixed aromatic–naphthenic nature; 5—compounds of mixed naphthenic–aliphatic nature.

The equilibrium of SARA fractions is essential in the behavior of asphalt binder because the maltenes allow the proper state of fluidity/workability, and the asphaltenes ensure adhesion with aggregates [63,84,85]. Some specific trends that asphalt binders have according to the distribution of their SARA fractions are listed below [3,63,72,78,86,87]:

- If the amount of resins and asphaltenes increases, the asphalt binder exhibits a more solid-like state. As a result, it causes an increase in stiffness.

- If the amount of saturates and aromatics increases, the asphalt binder exhibits a more liquid-like state. As a result, it causes a decrease in stiffness.
- If the amount of aromatics and asphaltenes increases, the asphalt binder reaches better properties at high temperatures.
- If the resin content increases, the viscosity of the asphalt binder augments proportionally.
- Adequate amounts of saturates, aromatics, and asphaltenes provide an appropriate fluid state.
- A low asphaltene content improves the temperature sensitivity behavior.

In this way, it is evident that a delicate chemical equilibrium in the SARA fractions widely controls the engineering performance of asphalt binders. The preceding is particularly important because incorporating graphene-like materials alters the SARA fractions. Thus, it explains why GMABs exhibit such complicated behavior, which is difficult to understand only by using traditional laboratory protocols. Subsequent sections of this manuscript detail the characteristics and properties of GMABs.

The further substantial effect that graphene-like materials have in asphalt binders is that the introduction of these additives prevents the oxidation aging mechanism (by extending the diffusion path of the gas) [88–91]. Notably, oxidation is the mechanism by which atmospheric oxygen diffuses throughout the asphalt matrix [63,92,93]. In turn, when the oxygen reaches the organic molecules of the asphalt binder, three chemical changes are assembled: fragmentation, oxygen addition, and condensation [92,94]. First, the large molecules are broken during the fragmentation, producing the smaller ones [92,95]; thus, the proportion of molecules with high molecular weight is progressively diminished [69,96]. Subsequently, the oxygen addition corresponds to constituting new functional groups, such as carbonyl (C=O), sulfoxide (S=O), hydroxyl, acid, and ester [77,79,92,97]. Figure 3 shows the chemical structure of some of these functional groups. Finally, during the condensation (also called the carbonization process), the aromatic (benzylic carbon group) and the larger, weightier molecules are formed due to polyaromatic oxidation reactions [63,92,98–100]. Consequently, the oxidation mechanism causes an increase in the stiffness of the asphalt binder and a loss of its adhesion/cohesion properties, which make it brittle, thus promoting cracking failure [101–104].

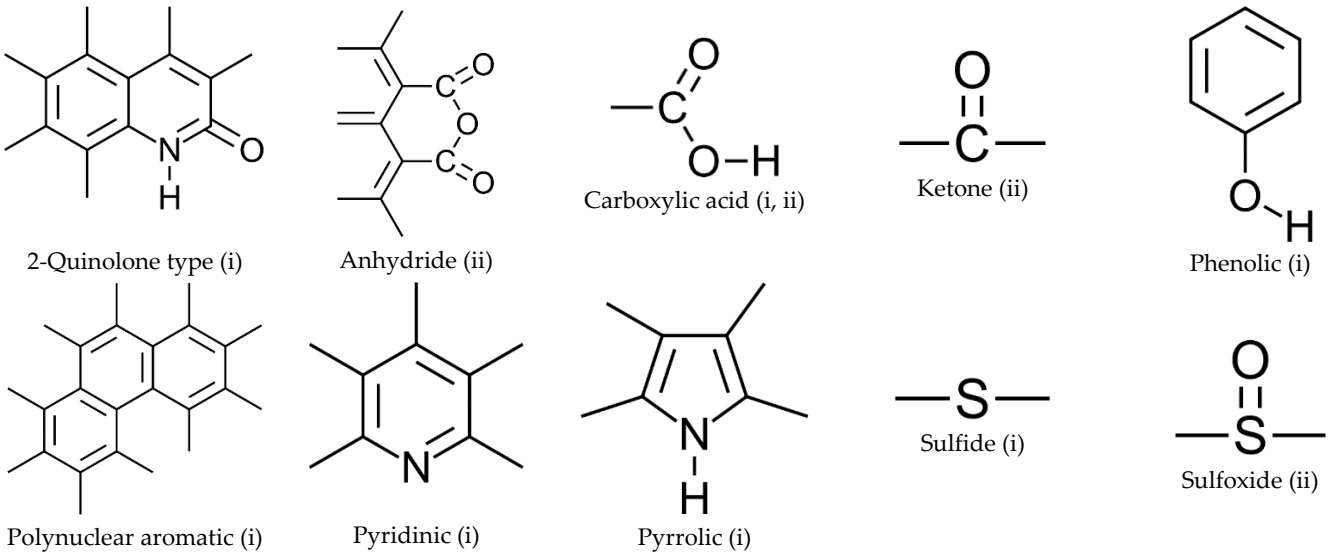

Figure 3. Functional groups formed during the oxidation aging mechanism. Adapted from [3]. Legend: (i) Naturally occurring; (ii) Induced by oxidation processes.

Consequently, it is notorious that the oxidation mechanism generates a complicated chain reaction of molecular rearrangements [3,105,106]. Furthermore, these reactions are

complex when asphalt binders are modified with graphene-like materials [31,32]. Therefore, in order to correctly characterize the GMABs, it is necessary to perform chemical, rheological, microstructural, morphological, thermogravimetric, and surface topography tests [34,53–55].

3. Basics of Graphene-like Materials

Despite being (correctly) isolated less than two decades ago (i.e., in 2004), graphene is a widespread substance with applications in dozens of heterogeneous industries (e.g., adsorption of pollutants, composite structures, detection of pesticides, combat against infectious diseases, lithium-ion battery manufacturing, membrane distillation, and wastewater treatment) [107–115]. Graphene can be defined as one of the allotropic forms of carbon, which has the shape of one thick atom layer of graphite [116–118]. Notably, the graphene's carbon atoms are organized as a honeycomb lattice with a network of delocalized π electrons [119–121]. In this way, graphene is an inorganic 2D nanomaterial hexagonally arranged in a structure through an sp2 hybridization [112,122,123]. Normally, graphene can be found in three forms: fullerene, nanotube, and graphite sheets [32,107]. On the other hand, graphene has many derivatives (also called "graphene family nanomaterials"), such as expanded graphite nanosheets, flake graphite, fluorographene, nanographite, reduced graphene oxide, graphane, graphene nanocomposites, graphene nanoribbon, graphene nanosheets, graphene quantum dots, graphone, and graphyne [124–127]. However, the most used (in different sectors) are the GO and GNPs [31,37,39,128,129].

The GO is the 2D material formed by oxidizing graphite, which is usually achieved with chemicals, such as sulphuric acid [33,51,88,91]. GO stands out over graphene and graphite because it has large amounts of surface functional groups, such as hydroxyl, carboxylic, and epoxy [31,40,130]. Moreover, unlike graphene, GO exhibits excellent dispersion in the aqueous solutions [18,40,131]. The preceding permits its correct blend and compatibility with the asphalt binder and other additives [18,35,52,132]. For instance, GO can promote the absorption of aromatics and saturates from SBS polymer to enhance the temperature response of the GMABs [30,31,51].

GNPs are platelet-like graphite nanocrystals formed by several graphene layers (usually less than ten) [10,32,133,134]. On the one hand, GNPs stand out over pure graphene and other derivatives due to a low production cost (at least regarding large-scale fabrication analysis) [133,135,136]. Furthermore, the GNPs exhibit a morphological characteristic of narrow distribution, an ultra-high aspect ratio, a significantly lighter weight, an ultra-high aspect ratio, a tensile strength of 101 GPa, and Young's modulus of 0.8–1 TPa [10,46,137]. Notably, GNPs develop an increased melting temperature and a low coefficient of thermal expansion that offers remarkable modifying-agent features [138–141]. Consequently, GNPs can be used at low concentrations to yield high-performance nanofluids [142–144].

Some main preparation methods for graphene-like materials are anodic bonding, chemical synthesis, using benzene as the building block, chemical vapor deposition process, growth from SiC, liquid phase exfoliation, micromechanical cleavage, molecular beam epitaxy, photoexfoliation, and precipitation from a carbon-containing metal substrate [29,32,145,146]. These preparation techniques can be classified as chemical preparation, physical preparation, micromechanical methods, and ultrasonic dispersion methods [32,34,39,147]. Regardless of the method employed for their preparation, the above nanomaterials present remarkable properties in common, i.e., elevated specific surface area, increased absorption, low bulk density, high functional density, great light transmittance, functional group-rich surfaces, and strong thermal-electrical conductivity [18,31,148]. Table 1 summarizes the main characteristics of these graphene-like materials. Due to these properties, graphene, GO, and GNPs have been used to modify asphalt binders [9,40]. In this way, the produced GMABs achieve a more extended service life with better performance (in comparison with a traditional unmodified asphalt binder) [31,32]. The subsequent section of this manuscript discusses the principal features of GMABs.

Table 1. Properties of main graphene-like materials.

Properties	Graphene	GO	GNPs	References
Appearance	Odorless black powder			[39,51,119]
Solubility in water	Negligible	Non-negligible		[119,149,150]
pH	8.3–11.4	Wildly variable		[119,151,152]
Number of layers	3–8	5–15	3–7	[18,35,40,51,133,153,154]
Diameter size, ⌀(μm)	11–18	5–100	1–15	[18,35,40,51,119,133,153]
Thickness (nm)	1–2	1–8	2–3	[18,35,40,51,133,153]
Specific surface area (m^2/g)	360	50–450	30–50	[18,35,39,40,51,153]
Bulk density (g/cm^3)	0.4	0.9–1.8	0.01–0.13	[39,119,155]
C content (wt.%)	100	60–75	99.5	[40,88,119]
O content (wt.%)	-	20–35		
S content (wt.%)	-	2		
Mn content (wt.%)	-	1	Negligible	[88,156,157]
K content (wt.%)	-	1		
Si content (wt.%)	-	1		

4. Properties of GMABs

Table 2 shows the effects of graphene-like materials on asphalt binder behavior. Overall, the GMABs present superior performance over traditional asphalt binders regarding fatigue and rutting resistances [31,32,90,158]. In this table, it is also evident that incorporating these nanomaterials causes the asphalt binder to increase its viscosity [18,147,155]. Because of this, GMABs used to require higher mixing temperatures (to produce asphalt mixtures) than conventional asphalt binders [39,50,88]. Likewise, the optimal binder content developed by GMABs is more elevated than the associated with neat asphalt binders [40,137,159,160].

Table 2. Effects of graphene-like materials on asphalt binder behavior. Adapted from [31,32,88,90,158].

Properties	Graphene	GO	GNPs
Aging resistance	↑	↑	↑
Density	↔	↔	↔
Ductility	↔	↓	↔
Fatigue resistance	↑	↑	↑
Flash point	↑	↑	↑
Loss modulus	↓	↔	↔
m value	↔	↔	↔
Moisture stability	↑	↑	↑
Penetration	↓	↓	↓
Recovery rate	↑	↑	↑
Rutting resistance	↑	↑	↑
Softening point	↑	↑	↑
Stifness modulus	↑	↑	↔
Storage modulus	↑	↔	↔
Thermal susceptibility	↓	↓	↓
Viscosity	↑	↑	↑

Legend: ↑ increment; ↓ reduction; ↔ no explicit trend.

GMABs have remarkable resistance to different aging processes, i.e., thermal, ultraviolet, and even water aging [21,30,89,90,161]. Nonetheless, the GMABs may exhibit increased volatilization of light components due to the high temperatures required for their production [3,162]. The preceding is associated with the large specific surface area of graphene-like

materials, which makes it difficult to disperse in some fluid media [31,32]. Notably, in order to facilitate the dispersion of graphene-like materials within the asphalt matrix, it is feasible to incorporate solvent or dispersant agents [119,163]. For instance, some common solvents are trichloroethylene and anhydrous ethanol [9,39,91,163]. Meanwhile, the dipropylene glycol dimethyl ether and polyvinyl pyrrolidone are typical dispersants [31,39,155]. Although there is still no total consensus in the literature, it is found as a majority trend that GO disperses more easily than graphene and GNPs [31,119]; this may be associated with the enriched number of oxygen-containing functional groups that the GO has [132,164].

Although the effects described in Table 2 are widely accepted in the literature, it is essential to clarify that the physicochemical properties of GMABs depend on the preparation process used to disperse and blend the graphene-like materials within the asphalt matrix [34,89,163]. There are three paramount manners for preparing GMABs, namely the direct addition method, the indirect addition method, and the auxiliary addition method [29,31,147]. These methods are described below [31–33,146]:

- Direct addition method: the graphene-like materials are directly added into the asphalt binder (previously elevated to a high temperature).
- Indirect addition method: the graphene-like materials and asphalt binder are simultaneously dissolved into a medium solution to subsequently form a uniform solution.
- Auxiliary addition method: the graphene-like materials are first altered by specific functional groups, and then, the new modifying agent is melted into the asphalt binder.

The graphene like-materials exhibit a large shape ratio (i.e., diameter/thickness), increased specific surface area, and scalable pore dimension [17,145,147,165]. Due to these properties, the geometry of the graphene-like materials controls the performance of the GMABs [49,50]. Notably, as the particle size of the modifying agent decreases, the GMABs increase their free volume fraction, glass transition temperature, and shear viscosity [18,83,128,138]. In other words, the particle geometry controls the low-temperature behavior and resistance to the permanent deformation [27,28,155,166,167]. Table 3 presents several case studies regarding GMABs and their performance. This table also includes information on graphene-like materials' particle geometry.

Table 3. Summary of case studies on GMABs.

References *	Neat Asphalt Binder **	Graphene-Like Material			Extra Modifying Agent
		Type	Geometry	Dosage (%)	
[9]	60/80 PNG	GO	⌀: 0.2–10 µm Thickness: 1–5 nm	0.06	Cross-linked chitosan, Glutaraldehyde, SBS
[10]	60/70 PNG	GNPs	⌀: 75 µm	0.5, 1, 1.5	-
[18]	60/70 PNG	GO	⌀: 10–50 µm Thickness: 1–1.77 nm	0.5, 1, 1.5, 2, 2.5	-
[27]	60/70 PNG	Graphene	⌀: <6 µm	2, 4, 6, 8, 10	-
[28]	60/70 PNG	GNPs	⌀: 5–10 µm Thickness: <3 nm	0.4	Polyethylene
[33]	60/70 PNG	GO	"not specified"	0.1, 0.3, 0.5, 0.7, 0.9	-
[52]	80/100 PNG	GO	⌀: 10–50 µm Thickness: 1 nm	0.2, 0.5, 1	Epoxy oligomer
[119]	PG 76–22	Graphene	⌀: 11 µm	0.3, 0.65, 1, 1.5, 2.5, 5, 7	SBS
[129]	60/80 PNG	GNPs	"not specified"	0.02, 0.08	Polystyrene, SBS
[130]	80/100 PNG	GO	"not specified"	0.5, 1	Polyurethane

Table 3. *Cont.*

References *	Neat Asphalt Binder **	Graphene-Like Material			Extra Modifying Agent
		Type	Geometry	Dosage (%)	
[131]	70/90 PNG	GO	⌀: 15–20 µm	0.5, 1, 1.5, 2	-
[137]	60/70 PNG	GNPs	⌀: 2–7 µm Thickness: 2–10 nm	2, 4	-
[147]	60/70 PNG	GO	Thickness: 50–80 nm	0.2, 0.4, 0.8, 1.6	Polyurethane
[155]	60/80 PNG	GNPs	⌀: 1–15 µm Thickness: 2.4 nm	0.5, 1, 1.5, 2	Polyvinylpyrrolidone, SBS
[158]	~80 PNG	Graphene	⌀: 5–50 µm Thickness: 3.4–8 nm	0.5, 1, 1.5	-
[163]	PG 64-22	Graphene	⌀: 7–15 µm	2–20	Ethylene bis(stearamide)
[165]	60/80 PNG	Graphene	⌀: 5–50 µm Thickness: 3.4–8 nm	2, 4, 5.9	Carbon fibers, Nickel
[166]	80/100 PNG	GNPs	⌀: 5–50 µm Thickness: 3.4–8 nm	0.5, 1, 1.5, 2	SBS
[168]	60/80 PNG	GO	⌀: 0.2–10 µm Thickness: 1–5 nm	0.02, 0.04, 0.06, 0.08	Fe^{3+}-TA, SBS

* In all case studies, a general improvement of mechanical properties was reported. ** PNG: penetration grade; PG: performance grade.

5. Characterization Techniques for GMABs

GMABs are usually initially characterized with a traditional test protocol, that is, the set of evaluations for density, penetration, softening point, dynamic viscosity, ductility, flash point, and solubility [4,10,18,21,32,46,49]. Nevertheless, these tests are insufficient to understand the thermo-dependent viscoelastic behavior of the GMABs [31,32]. For these purposes, it is necessary to resort to more advanced tests, such as AFM, DSC, DSR, EA, FTIR, RS, SEM, TGA, XRD, and XPS [4,21,32,49,169,170]; these are described below. In this way, it is possible to comprehensively assess chemical, rheological, microstructural, morphological, thermogravimetric, and surface topography properties. Moreover, these sophisticated tests allow to evaluate and ensure the correct dispersion of graphene-like materials within the structure of the asphalt matrix [119,158,171,172].

5.1. AFM

The AFM is a microscopy designed to record the topography of materials at a sub-nanometric scale for liquid and air media [173–176]. The AFM has been widely used to study GMABs [9,89,132]. The AFM employs a sharp-stylus probe to scan the material's surface by exploring the repulsive and attractive forces between the material and the probe [177–179]. In this way, a high-resolution dimensional topographic image in 2D or 3D is formed [49,89,166]. The analysis of these images (usually conducted with specialized software/algorithms) can yield additional information (not exclusive to the surface topography), such as adhesion forces, elasticity, electrostatic force, morphology, nanoindentation, nano-phase separation, roughness, and even stiffness [174,180,181]. The combined assessment of these properties can be utilized to identify changes in the asphalt binders' chemical structure [180,182,183]. For instance, through the identification of the three main phases of the asphalt binder morphology, i.e., catanaphase (bee structures), periphrases (dispersed phase), and paraphase (the matrix) [61,78,183–185]. Overall, the graphene-like materials can augment the number of "bee" structures in the structure of the asphalt binder but diminish their size [132,166].

5.2. DSR

The DSR is an apparatus utilized to measure the rheological response of some fluids under a wide range of temperatures, frequencies, and shear stress [19,186–189]. For instance, the DSR is typically used to examine the temperature-dependent viscoelastic behavior of asphalt binders, including GMBAs [166,188]. This device can record essential properties/parameters, such as complex modulus, complex viscosity, elastic modulus, phase angle, strain, stress, and viscous modulus [190,191]. Likewise, these results make it feasible to compute other vital parameters, such as zero shear viscosity, rutting factor, fatigue factor, non-recoverable compliance, and DSR function [192–194]. In the literature, it has been reported that the fatigue and rutting factors are especially sensitive to change after modifying the asphalt binder with graphene-like materials [46,137].

5.3. EA and XPS

The set of techniques employed to estimate the proportion of the chemical elements that contain a material is denominated EA [195–198]. Thus, the EA has commonly used to outline the chemical changes that an asphalt binder undergoes after its modification [67,199–201]. A wide range of devices and techniques exist to conduct an EA, even though XPS is the most utilized in the road infrastructure industry [202–204]. The preceding is because the XPS is efficient and versatile [3,205]. Overall, the XPS emits X-ray photons (with distinct energy) to excite electrons in the innermost orbitals of atoms [206,207]. Hence, a distinctive energy spectrum is generated, which contains peaks corresponding to the structure of the atoms found on the surface of the analyzed sample [204,208–210]. Consequently, it is easy to establish the chemical elements (and their proportions) that compose a material [211–213]. For instance, after modifying the asphalt binder with graphene-like materials, it is expected that the asphalt matrix will undergo an increase in the carbon ratio and a decrease in oxygen [53,214,215].

5.4. FTIR

The incorporation of graphene-like materials within the asphalt binder causes the asphalt matrix to alter the functional groups, i.e., some are transformed into new ones [9,37,169]. However, there is still no consensus regarding chemical reaction paths [89,130,146]. Notably, the chemistry of the GMABs will depend on the specific composition of the raw materials employed [29,34,161]. Therefore, in order to understand the changes suffered by the functional groups from a neat asphalt binder to a GMABs, it is necessary to carry out an FTIR analysis [28,90,166].

FTIR is a spectrometry method to estimate the capacity of a material to absorb light (infrared radiation) regarding a characteristic wavelength range [57,216]. Therefore, the FTIR computes the spectral bands, which are the brusque changes in the transmittance vs. the wavenumber [71,217,218]. Figure 4 shows a sketch of a typical plot from an FTIR analysis. In this way, since each functional group has a specific spectral band, it is feasible to calculate the proportion of one [44,219,220]. Although there are several approaches to calculating it, the most popular way is to divide the area under the curve centered on the specific spectral band of a functional group into the area under the curve of the entire spectrum evaluated [161,190,221]. It is important to note that the FTIR has a central problem: there is no unanimity on the specific wavenumbers and the entire spectral band to be considered [3,216]. The preceding can be evidenced in Table 4. This table presents the wavenumbers and spectral bands used to compute the functional group indexes in some case studies for C=O, S=O, aromatic, and butadiene groups. Thus, the proper producibility and replicability of the results could be affected.

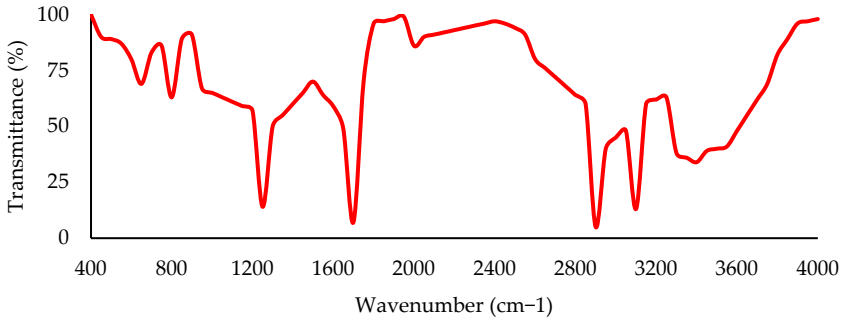

Figure 4. Typical graph of an FTIR analysis conducted in an asphalt binder sample. Adapted from [3].

Table 4. Wavenumbers and spectral bands used to compute the functional group indexes. Adapted from [3].

Functional Group	Distinctive Wavenumber (cm^{-1})	Total Spectral Band Evaluated (cm^{-1})	References
C=O	around 1600	600 to 2000	[222]
	around 1694	600 to 2000	[44]
	around 1700	725 to 3570	[223]
	around 1702	722 to 2920	[218]
S=O	around 1015	725 to 3570	[223]
	around 1027	600 to 2000	[44]
	around 1030	500 to 4000	[224]
	around 1032	723 to 2924	[71,217]
Aromatic	around 1600	723 to 2924	[220]
	around 1601	600 to 2000	[60,225]
	around 1601	723 to 2924	[71,217]
	around 1606	725 to 3570	[223]
Butadiene	around 966	600 to 2000	[222,226,227]
	around 966	722 to 2920	[218]
	around 968	600 to 2000	[228]
	around 985	600 to 2000	[229]

5.5. RS

As its name indicates, the RS is a spectroscopy technique that emits/relies upon Raman scattering (i.e., inelastic scattering of photons) in a specific (monochromatic) electromagnetic spectrum [230,231]. Usually, the RS devices detect and measure the vibration changes (scrolling up and down) in the system produced by the energy of the laser photons [232,233]. With this procedure, it is possible to deeply study a sample and, thus, obtain a "fingerprint" for each molecule [234,235]. In other words, RS allows the identification of the presence (in its quantity) of particular chemical compounds with high precision [236–238]. For the specific case of the GMABs, it is feasible to determine the content of graphene derivatives (i.e., carbonous materials) and their number of layers [169,239,240]. Consequently, the carbon molecules' diffusion degree (or coupling) within the GMABs can be estimated [241,242]. Although there is no consensus on the spectral range to be employed with GMABs, it is typical to consider a range between 800–2000 cm^{-1} [146,169]. Undoubtedly, it is expected that the amount of carbon molecules will increase remarkably after modifying the asphalt binder with graphene-like materials [54,243].

5.6. SEM

The SEM is a method for scanning and analyzing the microscopic morphology of organic and inorganic materials [244,245]. The resolution of the SEM tests can vary from micrometer to nanometer scale [246,247]. Overall, the SEM applies backscattered and low-energy secondary electrons to estimate the changes in the topography of a material's

surface [248,249]. Therefore, it is feasible to generate 3D images exhibiting the microstructural characteristics of the sample [250,251]. Although the results of SEM tests on GMABs may vary depending on the modifying agent used, it is almost considered by consensus that graphene-like materials cause the asphalt binder to develop a multilayer stacked flake structure with smooth and flat surface similar to crystal stone-like grooves [9,90,155,167].

5.7. TGA and DSC

The GMABs can develop complex thermal stability, varying over time [43,166]. Although there is no consensus on this criterion, thermal stability can be assessed by employing a TGA [252,253]. The TGA is a method that evaluates sample mass changes during a gradual temperature increase (even up to 1600 °C) [254–257]. Therefore, this test permits estimating different parameters related to the activation energy, decomposition, reaction kinetics, resistance to pyrolysis, and thermal behavior [252,258–260]. For asphalt binders, it is typical to draw a curve of temperature augments vs. mass lost ratio and then look for abrupt or accelerated changes (low thermal stability is evidenced with very noticeable changes) [252,253,261]. Notably, there is a wide range of TGA protocols; however, the DSC is the most widely used for petroleum-derived products [180,262–265]. The DSC stands out because it is the only direct method that allows estimating the enthalpy of a process and also indicates correlations between the physical properties of substances with their thermal behaviors [266–268]. Remarkably, the glass transition temperature is the most advantageous parameter for examining asphalt binders utilizing the DSC analysis [27,37,52]. This temperature is the middle point where the glass transition appears [26,60].

5.8. XRD

After modifying an asphalt binder with graphene-like materials, the asphalt matrix develops high quantities of new crystal structures [9,49,158]. Accordingly, one way to measure the degree of coupling between the molecules of the asphalt binder with molecules of the modifying agent is to evaluate the formation of crystalline structures [42,162,269,270]. Moreover, adding graphene-like materials diminishes the oxygen- containing functional groups (especially on the structural layer of carbon atoms) [9,32,48]. The preceding can be conducted through the XRD technique [271–273]. An XRD device implements X-rays (i.e., high-energy electromagnetic energy with low wavelengths) to emit photons directly to a sample [274–276]. Then, the XRD measures and follows the diffraction patterns and peaks [146,241]. In this way, it is possible to obtain data c ng the atomic structure of a specific material [163,277]. Likewise, examining the position of atoms and their arrangement is also feasible [278,279]. Notably, because this is a non-destructive test, the XRD has been used in various industries to study sensitive materials [280,281].

5.9. Summary of Characterization Techniques

Table 5 summarizes several investigations in which the preceding characterization techniques were implemented to analyze asphalt binders. Specifically, this table presents the central findings of various case studies on GMABs. In this way, each graphene-like material's main effects on the behavior and performance of the asphalt binders are exhibited. Additionally, Figure 5 shows a schematic explication of each of these devices.

Table 5. Summary of case studies on the analysis of GMABs with advanced characterization techniques.

Characterization Technique	Modifying Agent	Neat Asphalt Binder	Main Findings	References
AFM	Graphene	60/80 PNG	The graphene promotes the nucleation of bee structures, which augments the number and reduces the volume of these structures.	[55]
	GO	40/50 PNG	The GO causes a grafting reaction that yields wavy bends with a wide degree of curling.	[89]
	GNPs	60/80 PNG	THE AFM force curve analysis shows that GNPs reduce temperature sensibility and enhance plasticity and viscosity behavior.	[49]
DSR	Graphene	60/70 PNG	As the graphene content increases, the asphalt binder increases its viscosity and reduces its high-temperature susceptibility.	[27]
	GO	60/70 PNG	GO can greatly elevate the permanent deformation resistance of asphalt binders in a wide range of temperatures.	[35]
	GNPs	60/80 PNG	The GNPs inclusion enhances the high-temperature rutting resistance performance and the fatigue resistance.	[49]
EA and XPS	Graphene	40/50 PNG	The GMABs show three distinctive functional groups: nonoxygenated C-C (285.08 ev), ether C-0 (286.43 eV), and C=N bond (280 ev).	[282]
	GO	40/50 PNG	The strongest peaks caused by the GO were at 284.79, 286.61, 287.28, and 288.86 eV, representing C–C, C–O–Si, C–SH, and HO–C=O, respectively.	[89]
	GNPs	40/50 PNG	Regarding the GO, GNPs reduce the interplanar spacing of modified asphalt binder by approximately 48%.	[89]
FTIR	Graphene	40/60 PNG	The graphene yields anti-aging properties to the asphalt binder, at least in the spectral range of 1760–1500 cm^{-1}.	[169]
	GO	40/50 PNG	The more substantial absorption peaks were at 3386.6 and 1375.7 cm^{-1}, representing the hydroxyl group stretching and bending oscillation.	[89]
	GNPs	60/80 PNG	The GNPs modification was highlighted by characteristic absorption peaks at 1184.44, 1601.02, 1492.61, 1450.95, 755.12, and 698.43 cm^{-1}.	[49]
RS	Graphene	40/60 PNG	The G-band (1580 cm^{-1}) and the D-band (1350 cm^{-1}) can assess the presence of graphene.	[169]
	GO	70/100 PNG	GO modification is characterized by distinctive D and G peaks at 1352 cm^{-1} and 1600 cm^{-1}, respectively.	[17]
	GNPs	PG 58-28	The modification with GNPs provokes the prominent peaks: D-peak (1330 cm^{-1}), G-peak (1580 cm^{-1}), and 2D-peak (2660 cm^{-1}).	[283]
SEM	Graphene	40/50 PNG	The graphene provokes a microcrack propagation path, easily distinguished through this technique.	[282]
	GO	40/50 PNG	The GO yields a clear sheet structure with a smooth surface.	[89]
	GNPs	60/80 PNG	GNPs develop notorious small wrinkles and ellipsoidal structures.	[49]
TGA and DSC	Graphene	40/60 PNG	The presence of graphene causes the asphalt binder to increase its maximum degradation temperature and melting peaks.	[169]
	GO	60/80 PNG	GO can considerably enhance the thermal stability of asphalt binders.	[168]
	GNPs	PG 52-34	The modified asphalt binder reduces the susceptibility to moisture damage and increases the stiffness and resistance to failure conditions.	[284]
XRD	Graphene	60/80 PNG	Graphene develops a multilayered morphology with a peak centred at approximately 24°.	[158]
	GO	40/50 PNG	The GO generates a grafting process, which is easily identified by an interplanar spacing of 0.421 nm.	[89]
	GNPs	60/80 PNG	XRD pattern analysis demonstrates that the asphalt binder molecules increased the interlayer distance of GNPs.	[155]

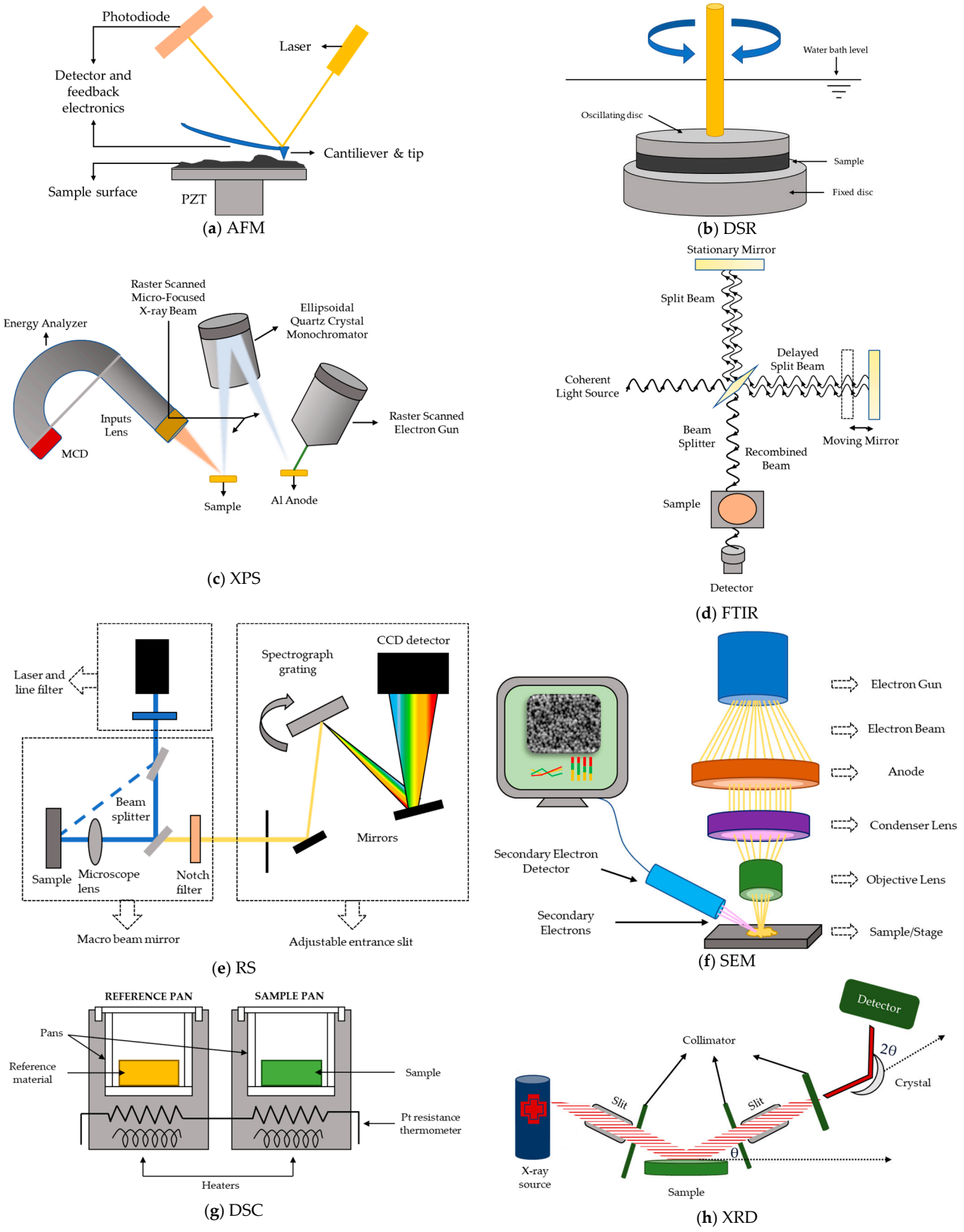

Figure 5. Schematic description of the functioning of the leading advanced characterization techniques for GMABs. Adapted from [285–292].

6. Discussion

Current investigation trends show that the researchers focus on applying optical techniques to study GMABs. Although these techniques are extremely useful for performing the physical–chemical characterizations of different materials, these laboratory protocols also can present significant disturbances and errors in the result reports [293,294]. Notably, optical-type techniques (basically all varieties of microscopy and spectroscopy) employ light (i.e., photochemistry, luminescence, and light scattering) to probe or manipulate materials [295,296]. Unfortunately, small changes in the conditions (both external and internal) of the test can greatly influence the observations and measurements recorded [297,298]. Thus, disturbances or inconsistencies in the execution and post-processing of the tests may impair the reliability of the results [299,300]. Accordingly, the test outcomes depend on the sample preparation quality and the skills of the laboratory worker (i.e., control over the environment, mastery over the test apparatus, and the ability to interpret the results) [301,302]. Even though more of these aspects cannot be easily handled, there is one that can be, that is, the data post-processing [303,304]. Researchers' main difficulty when using these optical techniques is interpreting the resultant images/photography manually [305,306]. Fortunately, this can be addressed by employing computational methods, such as artificial neural networks [245,250]. By implementing this type of artificial intelligence, it is feasible to analyze images in detail and find patterns, arrangements, and changes that could be effortlessly ignored (if they are done traditionally) [236,247]. Nonetheless, in the literature review, no research was found using machine learning to examine the test results on GMABs. The preceding represents an important gap in the literature.

On the other hand, another critical gap was evidenced in the literature: the tests on asphalt binders are usually conducted only before (i.e., on neat asphalt binders) and after (i.e., on GMABs) the modification processes. In this way, it is not common for the researchers to evaluate the properties of the GMABs over time, e.g., after several months of modifying the binder. The preceding implies that in the current state-of-the-art, there is no consensus on how the physical–chemical properties of the GMABs evolve in the long term. Consequently, this scenario is disturbing because the average service life of traditional asphalt pavements is 20 years, while it is 50 years in the case of perpetual pavements [12,307–310]. In other words, existing research trends do not permit knowing how GMABs would behave when used for road infrastructure construction. Notably, [55,90,161] evaluated the aging of the GMABs using the rolling thin film oven test, pressure-aging vessel test, and ultraviolet lamps. However, although these research efforts are not comparable to real-time long-term measurements [3,311], they demonstrate that some case studies have identified the need to carry out this type of assessment.

7. Future Research Lines

In light of the above, the current state-of-the-art about graphene-like materials and their applications to produce GMABs is susceptible to improvement. Therefore, some suggestions for future research lines are presented below: (i) implement machine learning to interpret the results obtained through advanced characterization techniques; (ii) research the physical–chemical change of the GMABs over the long term; (iii) develop mathematical–computational models to predict the effect of graphene-like materials on the asphalt binder performance; (iv) establish boundaries about the optimal geometric features that the graphene-like materials should have to guarantee the better possible behavior; and (v) evaluate the viability of other graphene derivatives, such as expanded graphite nanosheets, flake graphite, fluorographene, graphane, graphene nano-composites, graphene nanoribbon, graphene nanosheets, graphene quantum dots, graphone, graphyne, nanographite, and reduced graphene oxide.

8. Conclusions

In this research, a comprehensive literature review on the properties and characterization techniques of GMABs was carried out. Likewise, the main physicochemical aspects of

asphalt binders and graphene-like materials were explored and discussed. In this way, it was possible to draw the following conclusions:

- Neat asphalt binders are modified with graphene-like materials to produce high-performance binders.
- The prominent advantages of GMABs over traditional asphalt binders are decreased thermal susceptibility and increased resistance to aging, fatigue, rutting, and moisture damage.
- The primary graphene-like materials are used to modify asphalt binders are graphene, GO, and GNPs.
- The main processes for producing GMABs are the direct addition method, indirect addition method, and auxiliary addition method.
- GMABs are highly compatible with a wide variety of additional modifying agents, such as carbon fibers, cross-linked chitosan, crumb rubber, electric arc furnace slag, epoxy resins, ethylene bis(stearamide), Fe^{3+}-TA, glutaraldehyde, nickel, polyethylene, polystyrene, polyurethane, polyvinylpyrrolidone, and SBS.
- Conventional laboratory tests (i.e., density, penetration, softening point, dynamic viscosity, ductility, flash point, and solubility) are insufficient to characterize the complex behavior of GMABs. Therefore, it is necessary to employ advanced characterization techniques.
- In order to properly characterize the GMABs, it is essential to conduct assessments regarding chemical, rheological, microstructural, morphological, thermogravimetric, and surface topography properties. Notably, AFM, DSC, DSR, EA, FTIR, RS, SEM, TGA, XRD, and XPS are the leading tests for these purposes.
- There is still no consensus in the literature on the physicochemical properties of GMABs and their performance as a material for the road infrastructure industry. Regardless, all cutting-edge evaluation techniques indicate an improvement in low- and high-temperature performance (regarding the neat asphalt binders).
- Two primary gaps in the literature were identified: (i) although most of the advanced characterization techniques for GMABs are based on optical methods, researchers do not use computational approaches (such as artificial neural networks) to automatize the data interpretation process, and thus, reduce the inaccuracies associated with these observations/measurements; and (ii) not enough research efforts have been carried out to understand the behavior of the GMABs in the long-term.

Author Contributions: Conceptualization, R.P.-M.; methodology, T.N.-D.; validation, R.P.-M. and E.T.; formal analysis, D.O.-M.; investigation, T.N.-D.; data curation, D.O.-M.; writing—original draft preparation, R.P.-M.; writing—review and editing, T.N.-D., D.O.-M., E.T., G.M.-A. and R.P.-N.; visualization, T.N.-D. and D.O.-M.; supervision, R.P.-N.; project administration, G.M.-A. All authors have read and agreed to the published version of the manuscript.

Funding: This research received no external funding.

Data Availability Statement: Data is contained within this article.

Conflicts of Interest: The authors declare no conflict of interest.

References

1. Abudinen, D.; Fuentes, L.G.; Carvajal Muñoz, J.S. Travel Quality Assessment of Urban Roads Based on International Roughness Index: Case Study in Colombia. *Transp. Res. Rec.* **2017**, *2612*, 1–10. [CrossRef]
2. Fuentes, L.; Camargo, R.; Arellana, J.; Velosa, C.; Martinez-Arguelles, G. Modelling Pavement Serviceability of Urban Roads Using Deterministic and Probabilistic Approaches. *Int. J. Pavement Eng.* **2019**, *22*, 77–86. [CrossRef]
3. Polo-Mendoza, R.; Martinez-Arguelles, G.; Walubita, L.F.; Moreno-Navarro, F.; Giustozzi, F.; Fuentes, L.; Navarro-Donado, T. Ultraviolet Ageing of Bituminous Materials: A Comprehensive Literature Review from 2011 to 2022. *Constr. Build. Mater.* **2022**, *350*, 128889. [CrossRef]
4. Li, J.; Duan, S.; Muhammad, Y.; Yang, J.; Meng, F.; Zhu, Z.; Liu, Y. Microwave Assisted Fabrication of Polymethyl Methacrylate-Graphene Composite Nanoparticles Applied for the Preparation of SBS Modified Asphalt with Enhanced High Temperature Performance. *Polym. Test.* **2020**, *85*, 106388. [CrossRef]

5. Jin, L.; Zhang, Z.; Song, J. Profit Allocation and Subsidy Mechanism for Public-Private Partnership Toll Road Projects. *J. Manag. Eng.* **2020**, *36*, 04020011. [CrossRef]
6. Suprayoga, G.B.; Bakker, M.; Witte, P.; Spit, T. A Systematic Review of Indicators to Assess the Sustainability of Road Infrastructure Projects. *Eur. Transp. Res. Rev.* **2020**, *12*, 1–15. [CrossRef]
7. Welde, M.; Odeck, J. Cost Escalations in the Front-End of Projects-Empirical Evidence from Norwegian Road Projects. *Transp. Rev.* **2017**, *37*, 612–630. [CrossRef]
8. Toriola-Coker, L.O.; Alaka, H.; Agbali, M.; Bello, W.A.; Pathirage, C.; Oyedele, L. Marginalization of End-User Stakeholder's in Public Private Partnership Road Projects in Nigeria. *Int. J. Constr. Manag.* **2020**, *22*, 2098–2107. [CrossRef]
9. Huang, J.; Liu, Y.; Muhammad, Y.; Li, J.Q.; Ye, Y.; Li, J.; Li, Z.; Pei, R. Effect of Glutaraldehyde-Chitosan Crosslinked Graphene Oxide on High Temperature Properties of SBS Modified Asphalt. *Constr. Build. Mater.* **2022**, *357*, 129387. [CrossRef]
10. Eisa, M.S.; Mohamady, A.; Basiouny, M.E.; Abdulhamid, A.; Kim, J.R. Laboratory Evaluation of Mechanical Properties of Modified Asphalt and Mixture Using Graphene Platelets (GnPs). *Materials* **2021**, *14*, 5599. [CrossRef]
11. Polo-Mendoza, R.; Peñabaena-Niebles, R.; Giustozzi, F.; Martinez-Arguelles, G. Eco-Friendly Design of Warm Mix Asphalt (WMA) with Recycled Concrete Aggregate (RCA): A Case Study from a Developing Country. *Constr. Build. Mater.* **2022**, *326*, 126890. [CrossRef]
12. Walubita, L.F.; Martinez-Arguelles, G.; Polo-Mendoza, R.; Ick-Lee, S.; Fuentes, L. Comparative Environmental Assessment of Rigid, Flexible, and Perpetual Pavement: A Case Study of Texas. *Sustainability* **2022**, *14*, 9983. [CrossRef]
13. Polo-Mendoza, R.; Martinez-Arguelles, G.; Peñabaena-Niebles, R. A Multi-Objective Optimization Based on Genetic Algorithms for the Sustainable Design of Warm Mix Asphalt (WMA). *Int. J. Pavement Eng.* **2022**, 1–21. [CrossRef]
14. Plati, C. Sustainability Factors in Pavement Materials, Design, and Preservation Strategies: A Literature Review. *Constr. Build. Mater.* **2019**, *211*, 539–555. [CrossRef]
15. Li, J.; Xiao, F.; Zhang, L.; Amirkhanian, S.N. Life Cycle Assessment and Life Cycle Cost Analysis of Recycled Solid Waste Materials in Highway Pavement: A Review. *J. Clean. Prod.* **2019**, *233*, 1182–1206. [CrossRef]
16. Wang, H.; Liu, X.; Apostolidis, P.; Scarpas, T. Review of Warm Mix Rubberized Asphalt Concrete: Towards a Sustainable Paving Technology. *J. Clean. Prod.* **2018**, *177*, 302–314. [CrossRef]
17. Moreno-Navarro, F.; Sol-Sánchez, M.; Gámiz, F.; Rubio-Gámez, M.C. Mechanical and Thermal Properties of Graphene Modified Asphalt Binders. *Constr. Build. Mater.* **2018**, *180*, 265–274. [CrossRef]
18. Adnan, A.M.; Lü, C.; Luo, X.; Wang, J. Impact of Graphene Oxide on Zero Shear Viscosity, Fatigue Life and Low-Temperature Properties of Asphalt Binder. *Materials* **2021**, *14*, 3073. [CrossRef]
19. Turbay, E.; Martinez-Arguelles, G.; Navarro-Donado, T.; Sanchez-Cotte, E.; Polo-Mendoza, R.; Covilla-Valera, E. Rheological Behaviour of WMA-Modified Asphalt Binders with Crumb Rubber. *Polymers* **2022**, *14*, 4148. [CrossRef]
20. Ren, Y.-X.; Hao, P.W. Low-Temperature Performance of Asphalt Mixtures Modified by Microencapsulated Phase Change Materials with Various Graphene Contents. *Coatings* **2022**, *12*, 287. [CrossRef]
21. Guo, T.; Fu, H.; Wang, C.; Chen, H.; Chen, Q.; Wang, Q.; Chen, Y.; Li, Z.; Chen, A. Road Performance and Emission Reduction Effect of Graphene/Tourmaline-Composite-Modified Asphalt Tengteng. *Sustainability* **2021**, *13*, 8932. [CrossRef]
22. Perucca, M.; Capuano, L.; Magatti, G.; Rosa, F.; Mantecca, P. Environmental Performance of Road Asphalts Modified with End-of-Life Hard Plastics and Graphene: Strategies for Improving Sustainability. *Processes* **2022**, *10*, 2151. [CrossRef]
23. Xu, F.; Zhao, Y.; Li, K. Using Waste Plastics as Asphalt Modifier: A Review. *Materials* **2022**, *15*, 110. [CrossRef]
24. Li, Y.; Hao, P.; Zhao, C.; Ling, J.; Wu, T.; Li, D.; Liu, J.; Sun, B. Anti-Rutting Performance Evaluation of Modified Asphalt Binders: A Review. *J. Traffic Transp. Eng.* **2021**, *8*, 339–355. [CrossRef]
25. Al Hawesah, H.; Sadique, M.; Harris, C.; Al Nageim, H.; Stopp, K.; Pearl, H.; Shubbar, A. A Review on Improving Asphalt Pavement Service Life Using Gilsonite-Modified Bitumen. *Sustainability* **2021**, *13*, 6634. [CrossRef]
26. Behnood, A.; Modiri Gharehveran, M. Morphology, Rheology, and Physical Properties of Polymer-Modified Asphalt Binders. *Eur. Polym. J.* **2019**, *112*, 766–791. [CrossRef]
27. Yang, L.; Zhou, D.; Kang, Y. Rheological Properties of Graphene Modified Asphalt Binders. *Nanomaterials* **2020**, *10*, 2197. [CrossRef]
28. Zhou, H.-Y.; Dou, H.-B.; Chen, X.-H. Rheological Properties of Graphene/Polyethylene Composite Modified Asphalt Binder. *Materials* **2021**, *14*, 3986. [CrossRef] [PubMed]
29. Lu, Y.; Shi, N.; Wang, M.; Wang, X.; Yin, L.; Xu, Q.; Zhao, P. Research on the Preparation of Graphene Quantum Dots/SBS Composite-Modified Asphalt and Its Application Performance. *Coatings* **2022**, *12*, 515. [CrossRef]
30. Li, S.; Xu, W.; Zhang, F.; Wu, H.; Ge, Q. Effect of Graphene Oxide on Aging Properties of Polyurethane-SBS Modified Asphalt and Asphalt Mixture. *Polymers* **2022**, *14*, 3496. [CrossRef]
31. He, J.; Hu, W.; Xiao, R.; Wang, Y.; Polaczyk, P.; Huang, B. A Review on Graphene/GNPs/GO Modified Asphalt. *Constr. Build. Mater.* **2022**, *330*, 127222. [CrossRef]
32. Han, M.; Muhammad, Y.; Wei, Y.; Zhu, Z.; Huang, J.; Li, J. A Review on the Development and Application of Graphene Based Materials for the Fabrication of Modified Asphalt and Cement. *Constr. Build. Mater.* **2021**, *285*, 122885. [CrossRef]
33. Zeng, Q.; Liu, Y.; Liu, Q.; Liu, P.; He, Y.; Zeng, Y. Preparation and Modification Mechanism Analysis of Graphene Oxide Modified Asphalts. *Constr. Build. Mater.* **2020**, *238*, 117706. [CrossRef]

34. Su, Z.; Muhammad, Y.; Sahibzada, M.; Li, J.; Meng, F.; Wei, Y.; Zhao, Z.; Zhang, L. Preparation and Properties of Aminated Graphene Fiber Incorporated Modified Asphalt. *Constr. Build. Mater.* **2019**, *229*, 116836. [CrossRef]
35. An, X.; Wang, R.; Kang, X.; Yue, J. A More Accurate Fatigue Characterization of GO-Modified Asphalt Binder Considering Non-Linear Viscoelastic Behaviour and UV Exposure Effects. *Int. J. Fatigue* **2023**, *168*, 107396. [CrossRef]
36. Li, S.; Xu, W.; Zhang, F.; Wu, H.; Zhao, P. Effect of Graphene Oxide on the Low-Temperature Crack Resistance of Polyurethane-SBS-Modified Asphalt and Asphalt Mixtures. *Polymers* **2022**, *14*, 453. [CrossRef] [PubMed]
37. Li, K.; Ren, H.; Huang, W. Effect of Graphene Nanoplatelets (GNPs) on Fatigue Properties of Asphalt Mastics. *Materials* **2021**, *14*, 4864. [CrossRef]
38. Gulisano, F.; Crucho, J.; Gallego, J.; Picado-Santos, L. Microwave Healing Performance of Asphalt Mixture Containing Electric Arc Furnace (EAF) Slag and Graphene Nanoplatelets (GNPs). *Appl. Sci.* **2020**, *10*, 1428. [CrossRef]
39. Huang, G.; He, J.; Zhang, X.; Feng, M.; Tan, Y.; Lv, C.; Huang, H.; Jin, Z. Applications of Lambert-Beer Law in the Preparation and Performance Evaluation of Graphene Modified Asphalt. *Constr. Build. Mater.* **2021**, *273*, 121582. [CrossRef]
40. Adnan, A.M.; Luo, X.; Lü, C.; Wang, J.; Huang, Z. Improving Mechanics Behavior of Hot Mix Asphalt Using Graphene-Oxide. *Constr. Build. Mater.* **2020**, *254*, 119261. [CrossRef]
41. Asim, N.; Badiei, M.; Samsudin, N.A.; Mohammad, M.; Razali, H.; Soltani, S.; Amin, N. Application of Graphene-Based Materials in Developing Sustainable Infrastructure: An Overview. *Compos. Part B Eng.* **2022**, *245*, 110188. [CrossRef]
42. Fakhri, M.; Shahryari, E. The Effects of Nano Zinc Oxide (ZnO) and Nano Reduced Graphene Oxide (RGO) on Moisture Susceptibility Property of Stone Mastic Asphalt (SMA). *Case Stud. Constr. Mater.* **2021**, *15*, e00655. [CrossRef]
43. Li, Z.; Yu, X.; Liang, Y.; Wu, S. Carbon Nanomaterials for Enhancing the Thermal, Physical and Rheological Properties of Asphalt Binders. *Materials* **2021**, *14*, 2585. [CrossRef] [PubMed]
44. Omar, H.A.; Katman, H.Y.; Bilema, M.; Ahmed, M.K.A.; Milad, A.; Md Yusoff, N.I. The Effect of Ageing on Chemical and Strength Characteristics of Nanoclay-Modified Bitumen and Asphalt Mixture. *Appl. Sci.* **2021**, *11*, 6709. [CrossRef]
45. Ahmed, T.M.; Al-Khalid, H.; Ahmed, T.Y. Review of Techniques, Approaches and Criteria of Hot-Mix Asphalt Fatigue. *J. Mater. Civ. Eng.* **2019**, *31*, 03119004. [CrossRef]
46. Chen, Y.; Wang, Q.; Li, Z.; Ding, S. Rhysiological Properties of Graphene Nanoplatelets/Rubber Crowd Composite Modified Asphalt. *Constr. Build. Mater.* **2020**, *261*, 120505. [CrossRef]
47. Alamnie, M.M.; Taddesse, E.; Hoff, I. Advances in Permanent Deformation Modeling of Asphalt Concrete—A Review. *Materials* **2022**, *15*, 3480. [CrossRef]
48. Han, M.; Li, J.; Muhammad, Y.; Yin, Y.; Yang, J.; Yang, S.; Duan, S. Studies on the Secondary Modification of SBS Modified Asphalt by the Application of Octadecyl Amine Grafted Graphene Nanoplatelets as Modifier. *Diam. Relat. Mater.* **2018**, *89*, 140–150. [CrossRef]
49. Han, M.; Li, J.; Muhamma, Y.; Hou, D.; Zhang, F.; Yin, Y.; Duan, S. Effect of Polystyrene Grafted Graphene Nanoplatelets on the Physical and Chemical Properties of Asphalt Binder. *Constr. Build. Mater.* **2018**, *174*, 108–119. [CrossRef]
50. Gao, Y.; Xie, Y.; Liao, M.; Li, Y.; Zhu, J.; Tian, W. Study on the Mechanism of the Effect of Graphene on the Rheological Properties of Rubber-Modified Asphalt Based on Size Effect. *Constr. Build. Mater.* **2023**, *364*, 129815. [CrossRef]
51. Hu, K.; Yu, C.; Yang, Q.; Chen, Y.; Chen, G.; Ma, R. Multi–Scale Enhancement Mechanisms of Graphene Oxide on Styrene–Butadiene–Styrene Modified Asphalt: An Exploration from Molecular Dynamics Simulations. *Mater. Des.* **2021**, *208*, 109901. [CrossRef]
52. Zhang, J.; Wang, R.; Zhao, R.; Jing, F.; Li, C.; Wang, Q.; Xie, H. Graphene Oxide-Modified Epoxy Asphalt Bond Coats with Enhanced Bonding Properties. *Materials* **2022**, *15*, 6846. [CrossRef] [PubMed]
53. Wang, X.; Guo, Y.; Su, J.; Zhang, X.; Wang, Y.; Tan, Y. Fabrication and Characterization of Novel Electrothermal Self-Healing Microcapsules with Graphene/Polymer Hybrid Shells for Bitumenious Material. *Nanomaterials* **2018**, *8*, 419. [CrossRef]
54. Wang, R.; Fan, H.; Jiang, W.; Ni, G.; Qu, S. Amino-Functionalized Graphene Quantum Dots Prepared Using High-Softening Point Asphalt and Their Application in Fe^{3+} Detection. *Appl. Surf. Sci.* **2019**, *467–468*, 446–455. [CrossRef]
55. Li, X.; Wang, Y.; Wu, Y.; Wang, H.; Wang, Q.; Zhu, X.; Liu, X.; Sun, H.; Fan, L. Effect of Graphene on Modified Asphalt Microstructures Based on Atomic Force Microscopy. *Materials* **2021**, *14*, 3677. [CrossRef]
56. Peng, C.; Yu, J.; Dai, J.; Yin, J. Effect of Zn/Al Layered Double Hydroxide Containing 2-Hydroxy-4-n-Octoxy-Benzophenone on UV Aging Resistance of Asphalt. *Adv. Mater. Sci. Eng.* **2015**, *2015*, 739831. [CrossRef]
57. Hofko, B.; Porot, L.; Falchetto Cannone, A.; Poulikakos, L.; Huber, L.; Lu, X.; Mollenhauer, K.; Grothe, H. FTIR Spectral Analysis of Bituminous Binders: Reproducibility and Impact of Ageing Temperature. *Mater. Struct.* **2018**, *51*, 45. [CrossRef]
58. Mirwald, J.; Werkovits, S.; Camargo, I.; Maschauer, D.; Hofko, B.; Grothe, H. Understanding Bitumen Ageing by Investigation of Its Polarity Fractions. *Constr. Build. Mater.* **2020**, *250*, 118809. [CrossRef]
59. Mirwald, J.; Werkovits, S.; Camargo, I.; Maschauer, D.; Hofko, B.; Grothe, H. Investigating Bitumen Long-Term-Ageing in the Laboratory by Spectroscopic Analysis of the SARA Fractions. *Constr. Build. Mater.* **2020**, *258*, 119577. [CrossRef]
60. Hosseinnezhad, S.; Zadshir, M.; Yu, X.; Yin, H.; Sharma, B.K.; Fini, E. Differential Effects of Ultraviolet Radiation and Oxidative Aging on Bio-Modified Binders. *Fuel* **2019**, *251*, 45–56. [CrossRef]
61. Xing, C.; Liu, L.; Li, M. Chemical Composition and Aging Characteristics of Linear SBS Modified Asphalt Binders. *Energy Fuels* **2020**, *34*, 4194–4200. [CrossRef]

62. Liu, H.Y.; Zhang, H.L.; Hao, P.W.; Zhu, C.Z. The Effect of Surface Modifiers on Ultraviolet Aging Properties of Nano-Zinc Oxide Modified Bitumen. *Pet. Sci. Technol.* **2015**, *33*, 72–78. [CrossRef]
63. Tauste, R.; Moreno-Navarro, F.; Sol-Sánchez, M.; Rubio-Gámez, M.C. Understanding the Bitumen Ageing Phenomenon: A Review. *Constr. Build. Mater.* **2018**, *192*, 593–609. [CrossRef]
64. Cong, P.; Wang, X.; Xu, P.; Liu, J.; He, R.; Chen, S. Investigation on Properties of Polymer Modified Asphalt Containing Various Antiaging Agents. *Polym. Degrad. Stab.* **2013**, *98*, 2627–2634. [CrossRef]
65. Tang, N.; Yang, Y.L.; Yu, M.L.; Wang, W.L.; Cao, S.Y.; Wang, Q.; Pan, W.H. Investigation of Ageing in Bitumen Using Fluorescence Spectrum. *Materials* **2018**, *11*, 1325. [CrossRef]
66. Lyu, L.; Pei, J.; Hu, D.; Fini, E.H. Durability of Rubberized Asphalt Binders Containing Waste Cooking Oil under Thermal and Ultraviolet Aging. *Constr. Build. Mater.* **2021**, *299*, 124282. [CrossRef]
67. Mirwald, J.; Nura, D.; Hofko, B. Recommendations for Handling Bitumen Prior to FTIR Spectroscopy. *Mater. Struct.* **2022**, *55*, 26. [CrossRef]
68. Hu, J.; Wu, S.; Liu, Q.; García, M.; Zeng, W. Effect of Ultraviolet Radiation on Bitumen by Different Ageing Procedures. *Constr. Build. Mater.* **2018**, *163*, 73–79. [CrossRef]
69. Shi, H. Improvement of Polymers by UV Irradiation: The Research in Ageing and Solidification—Take Polysiloxane-Modified-Polyacrylates and Asphalt as AnExample. *Appl. Mech. Mater.* **2014**, *541–542*, 90–94. [CrossRef]
70. Rahimi, P.M.; Gentzis, T. Chapter 19: The Chemistry of Bitumen and Heavy Oil Processing. In *Practical Advances in Petroleum Processing*; Springer: New York, NY, USA, 2006; pp. 149–186.
71. Feng, Z.G.; Bian, H.J.; Li, X.J.; Yu, J.Y. FTIR Analysis of UV Aging on Bitumen and Its Fractions. *Mater. Struct.* **2015**, *49*, 1381–1389. [CrossRef]
72. Apostolidis, P.; Liu, X.; Kasbergen, C.; Scarpas, A.T. Synthesis of Asphalt Binder Aging and the State of the Art of Antiaging Technologies. *Transp. Res. Rec.* **2017**, *2633*, 147–153. [CrossRef]
73. Yu, M.; Wu, S.; Chen, M. Experimental Investigation of the Volatilization of Asphalts under Different Conditions. *Adv. Mater. Res.* **2012**, *463–464*, 69–75. [CrossRef]
74. Hung, A.M.; Fini, E.H. Absorption Spectroscopy to Determine the Extent and Mechanisms of Aging in Bitumen and Asphaltenes. *Fuel* **2019**, *242*, 408–415. [CrossRef]
75. Androjić, I. Ageing of Hot Mix Asphalt. *Gradjevinar* **2016**, *68*, 477–483. [CrossRef]
76. Kumar, A.; Choudhary, R.; Kumar, A. Aging Characteristics of Asphalt Binders Modified with Waste Tire and Plastic Pyrolytic Chars. *PLoS ONE* **2021**, *16*, e0256030. [CrossRef]
77. Lesueur, D. The Colloidal Structure of Bitumen: Consequences on the Rheology and on the Mechanisms of Bitumen Modification. *Adv. Colloid Interface Sci.* **2009**, *145*, 42–82. [CrossRef]
78. Ozdemir, D.K.; Topal, A.; McNally, T. Relationship between Microstructure and Phase Morphology of SBS Modified Bitumen with Processing Parameters Studied Using Atomic Force Microscopy. *Constr. Build. Mater.* **2021**, *268*, 121061. [CrossRef]
79. Fernández-Gómez, W.; Rondón, H.; Reyes, F. Effects of Aging by UV Radiation on Chemical and Rheological Properties of Asphalt Cements Extracted from Two Hot Mixed Asphalts. *Rev. ION* **2017**, *30*, 7–16. [CrossRef]
80. Zhao, Z.J.; Xu, S.; Wu, W.F.; Yu, J.Y.; Wu, S.P. The Aging Resistance of Asphalt Containing a Compound of LDHs and Antioxidant. *Pet. Sci. Technol.* **2015**, *33*, 787–793. [CrossRef]
81. Shishkova, I.; Stratiev, D.; Kolev, I.V.; Nenov, S.; Nedanovski, D.; Atanassov, K.; Ivanov, V.; Ribagin, S. Challenges in Petroleum Characterization—A Review. *Energies* **2022**, *15*, 7765. [CrossRef]
82. Yang, L.; Sheng, J.J. Experimental Study on the Oxidation Behaviors of Wolfcamp Light Crude Oil and Its Saturate, Aromatic and Resin Fractions Using Accelerated Rate Calorimetry Tests. *Fuel* **2020**, *276*, 117927. [CrossRef]
83. Porto, M.; Angelico, R.; Caputo, P.; Abe, A.A.; Teltayev, B.; Rossi, C.O. The Structure of Bitumen: Conceptual Models and Experimental Evidences. *Materials* **2022**, *15*, 905. [CrossRef]
84. Karahancer, S.; Enieb, M.; Saltan, M.; Terzi, S.; Eriskin, E.; Cengizhan, A.; Akbas, M.Y. Evaluating Mechanical Properties of Bitumen and Hot Mix Asphalt Modified with Nano Ferric Oxide. *Constr. Build. Mater.* **2020**, *234*, 117381. [CrossRef]
85. Sengoz, B.; Isikyakar, G. Analysis of Styrene-Butadiene-Styrene Polymer Modified Bitumen Using Fluorescent Microscopy and Conventional Test Methods. *J. Hazard. Mater.* **2008**, *150*, 424–432. [CrossRef]
86. Hunter, R.; Self, A.; Read, J. *The Shell Bitumen Handbook*, 6th ed.; Thomas Telford: London, UK, 2015.
87. Qian, C.; Fan, W. Evaluation and Characterization of Properties of Crumb Rubber/SBS Modified Asphalt. *Mater. Chem. Phys.* **2020**, *253*, 123319. [CrossRef]
88. Li, B.; Liu, P.; Zhao, Y.; Li, X.; Cao, G. Effect of Graphene Oxide in Different Phases on the High Temperature Rheological Properties of Asphalt Based on Grey Relational and Principal Component Analysis. *Constr. Build. Mater.* **2023**, *362*, 129714. [CrossRef]
89. Li, J.; Han, M.; Muhammad, Y.; Liu, Y.; Su, Z.; Yang, J.; Yang, S.; Duan, S. Preparation and Properties of SBS-g-GOs-Modified Asphalt Based on a Thiol-Ene Click Reaction in a Bituminous Environment. *Polymers* **2018**, *10*, 1264. [CrossRef]
90. Wu, S.; Zhao, Z.; Li, Y.; Pang, L.; Amirkhanian, S.; Riara, M. Evaluation of Aging Resistance of Graphene Oxide Modified Asphalt. *Appl. Sci.* **2017**, *7*, 702. [CrossRef]
91. Zeng, W.; Wu, S.; Pang, L.; Sun, Y.; Chen, Z. The Utilization of Graphene Oxide in Traditional Construction Materials: Asphalt. *Materials* **2017**, *10*, 48. [CrossRef]

92. Das, P.K.; Baaj, H.; Kringos, N.; Tighe, S. Coupling of Oxidative Ageing and Moisture Damage in Asphalt Mixtures. *Road Mater. Pavement Des.* **2015**, *16*, 265–279. [CrossRef]
93. Liu, Q.; Wu, J.; Xie, L.; Zhang, Z.; Ma, X.; Oeser, M. Micro-Scale Investigation of Aging Gradient within Bitumen Film around Air-Binder Interface. *Fuel* **2021**, *286*, 119404. [CrossRef]
94. Hu, D.; Gu, X.; Dong, Q.; Lyu, L.; Cui, B.; Pei, J. Investigating the Bio-Rejuvenator Effects on Aged Asphalt through Exploring Molecular Evolution and Chemical Transformation of Asphalt Components during Oxidative Aging and Regeneration. *J. Clean. Prod.* **2021**, *329*, 129711. [CrossRef]
95. Li, Y.; Li, H.; Nie, S.; Wu, S.; Liu, Q.; Li, C.; Shu, B.; Li, C.; Song, W.; Zou, Y.; et al. Negative Impacts of Environmental Factors (UV Radiation, Water and Different Solutions) on Bitumen and Its Mechanism. *Constr. Build. Mater.* **2020**, *265*, 120288. [CrossRef]
96. Chen, Z.; Zhang, H.; Duan, H. Investigation of Ultraviolet Radiation Aging Gradient in Asphalt Binder. *Constr. Build. Mater.* **2020**, *246*, 118501. [CrossRef]
97. Fernández-Gómez, W.; Rondón, H.; Reyes, F. A Review of Asphalt and Asphalt Mixture Aging. *Ing. Investig.* **2013**, *33*, 5–12. [CrossRef]
98. Das, P.K.; Balieu, R.; Kringos, N.; Birgisson, B. On the Oxidative Ageing Mechanism and Its Effect on Asphalt Mixtures Morphology. *Mater. Struct.* **2015**, *48*, 3113–3127. [CrossRef]
99. Osmari, P.; Leite, L.; Aragão, F.; Cravo, M.; Dantas, L.; Macedo, T. Cracking Resistance Evaluation of Asphalt Binders Subjected to Different Laboratory and Field Aging Conditions. *Road Mater. Pavement Des.* **2019**, *20*, S663–S677. [CrossRef]
100. Petersen, J.C. A Review of the Fundamentals of Asphalt Oxidation: Chemical, Physicochemical, Physical Property, and Durability Relationships. *TRB Transp. Res. Circ. E-C140* **2009**, 37–41.
101. Azarhoosh, A.; Abandansari, H.F.; Hamedi, G.H. Surface-Free Energy and Fatigue Performance of Hot-Mix Asphalt Modified with Nano Lime. *J. Mater. Civ. Eng.* **2019**, *31*, 04019192. [CrossRef]
102. Aguiar-Moya, J.P.; Salazar-Delgado, J.; Baldi-Sevilla, A.; Leiva-Villacorta, F.; Loria-Salazar, L. Effect of Aging on Adhesion Properties of Asphalt Mixtures with the Use of Bitumen Bond Strength and Surface Energy Measurement Tests. *Transp. Res. Rec.* **2015**, *2505*, 57–65. [CrossRef]
103. Cheng, D.; Little, D.N.; Lytton, R.L.; Holste, J.C. Surface Energy Measurement of Asphalt and Its Application to Predicting Fatigue and Healing in Asphalt Mixtures. *Transp. Res. Rec.* **2002**, *1810*, 44–53. [CrossRef]
104. Wei, J.; Zhang, Y. Influence of Aging on Surface Free Energy of Asphalt Binder. *Int. J. Pavement Res. Technol.* **2010**, *3*, 343–351.
105. Menapace, I.; Yiming, W.; Masad, E. Chemical Analysis of Surface and Bulk of Asphalt Binders Aged with Accelerated Weathering Tester and Standard Aging Methods. *Fuel* **2017**, *202*, 366–379. [CrossRef]
106. Lopes, M.; Zhao, D.; Chailleux, E.; Kane, M.; Gabet, T.; Petiteau, C.; Soares, J. Characterisation of Ageing Processes on the Asphalt Mixture Surface. *Road Mater. Pavement Des.* **2014**, *15*, 477–487. [CrossRef]
107. Rout, D.R.; Jena, H.M.; Baigenzhenov, O.; Hosseini-Bandegharaei, A. Graphene-Based Materials for Effective Adsorption of Organic and Inorganic Pollutants: A Critical and Comprehensive Review. *Sci. Total Environ.* **2023**, *863*, 160871. [CrossRef]
108. Loudiki, A.; Azriouil, M.; Matrouf, M.; Laghrib, F.; Farahi, A.; Saqrane, S.; Bakasse, M.; Lahrich, S.; El Mhammedi, M.A. Graphene-Based Electrode Materials Used for Some Pesticide's Detection in Food Samples: A Review. *Inorg. Chem. Commun.* **2022**, *144*, 109891. [CrossRef]
109. Dey, N.; Vickram, S.; Thanigaivel, S.; Kamatchi, C.; Subbaiya, R.; Karmegam, N.; Govarthanan, M. Graphene Materials: Armor against Nosocomial Infections and Biofilm Formation—A Review. *Environ. Res.* **2022**, *214*, 113867. [CrossRef]
110. Yu, S.; Guo, B.; Zeng, T.; Qu, H.; Yang, J.; Bai, J. Graphene-Based Lithium-Ion Battery Anode Materials Manufactured by Mechanochemical Ball Milling Process: A Review and Perspective. *Compos. Part B Eng.* **2022**, *246*, 110232. [CrossRef]
111. Seraj, S.; Mohammadi, T.; Tofighy, M.A. Graphene-Based Membranes for Membrane Distillation Applications: A Review. *J. Environ. Chem. Eng.* **2022**, *10*, 107974. [CrossRef]
112. Kumari, P.; Samadder, S.R. Valorization of Carbonaceous Waste into Graphene Materials and Their Potential Application in Water & Wastewater Treatment: A Review. *Mater. Today Chem.* **2022**, *26*, 101192. [CrossRef]
113. Zhang, L.; Chen, Z.; Habibi, M.; Ghabussi, A.; Alyousef, R. Low-Velocity Impact, Resonance, and Frequency Responses of FG-GPLRC Viscoelastic Doubly Curved Panel. *Compos. Struct.* **2021**, *269*, 114000. [CrossRef]
114. Moayedi, H.; Habibi, M.; Safarpour, H.; Safarpour, M.; Foong, L.K. Buckling and Frequency Responses of A Graphen Nanoplatelet Reinforced Composite Microdisk. *Int. J. Appl. Mech.* **2019**, *11*, 1950102. [CrossRef]
115. Al-Furjan, M.S.H.; Habibi, M.; Ghabussi, A.; Safarpour, H.; Safarpour, M.; Tounsi, A. Non-Polynomial Framework for Stress and Strain Response of the FG-GPLRC Disk Using Three-Dimensional Refined Higher-Order Theory. *Eng. Struct.* **2021**, *228*, 111496. [CrossRef]
116. Dąbrowski, B.; Żuchowska, A.; Brzózka, Z. Graphene Oxide Internalization into Mammalian Cells—A Review. *Colloids Surfaces B Biointerfaces* **2023**, *221*, 112998. [CrossRef] [PubMed]
117. Colmiais, I.; Silva, V.; Borme, J.; Alpuim, P.; Mendes, P.M. Towards RF Graphene Devices: A Review. *FlatChem* **2022**, *35*, 100409. [CrossRef]
118. Jiménez-Suárez, A.; Prolongo, G. Graphene Nanoplatelets. *Appl. Sci.* **2020**, *10*, 1753. [CrossRef]
119. Wang, Y.; Polaczyk, P.; He, J.; Lu, H.; Xiao, R.; Huang, B. Dispersion, Compatibility, and Rheological Properties of Graphene-Modified Asphalt Binders. *Constr. Build. Mater.* **2022**, *350*, 128886. [CrossRef]

120. Jena, G.; Philip, J. A Review on Recent Advances in Graphene Oxide-Based Composite Coatings for Anticorrosion Applications. *Prog. Org. Coatings* **2022**, *173*, 107208. [CrossRef]
121. Walunjkar, P.M.; Bajad, M.N. Review on Effect of Graphene Reinforcement on Properties of Cement Concrete. *Mater. Today Proc.* **2022**, 1–7. [CrossRef]
122. Gautam, R.; Marriwala, N.; Devi, R. A Review: Study of Mxene and Graphene Together. *Meas. Sensors* **2023**, *25*, 100592. [CrossRef]
123. Xu, Y.; Fu, K.; Liu, K.; Sun, K.; Dong, Y.; Yao, L. A State of the Art Review of the Tribology of Graphene/MoS2 Nanocomposites. *Mater. Today Commun.* **2023**, *34*, 105108. [CrossRef]
124. Torkaman-Asadi, M.A.; Kouchakzadeh, M.A. Atomistic Simulations of Mechanical Properties and Fracture of Graphene: A Review. *Comput. Mater. Sci.* **2022**, *210*, 111457. [CrossRef]
125. Saravanan, A.; Kumar, P.S.; Srinivasan, S.; Jeevanantham, S.; Vishnu, M.; Amith, K.V.; Sruthi, R.; Saravanan, R.; Vo, D.V.N. Insights on Synthesis and Applications of Graphene-Based Materials in Wastewater Treatment: A Review. *Chemosphere* **2022**, *298*, 134284. [CrossRef] [PubMed]
126. Gopika, G.; Sathish, A.; Kumar, P.S.; Nithya, K.; Rangasamy, G. A Review on Current Progress of Graphene-Based Ternary Nanocomposites in the Removal of Anionic and Cationic Inorganic Pollutants. *Chemosphere* **2022**, *309*, 136617. [CrossRef]
127. Ren, S.; Cui, M.; Liu, C.; Wang, L. A Comprehensive Review on Ultrathin, Multi-Functionalized, and Smart Graphene and Graphene-Based Composite Protective Coatings. *Corros. Sci.* **2023**, *212*, 110939. [CrossRef]
128. Tayouri, M.I.; Estaji, S.; Mousavi, S.R.; Salkhi Khasraghi, S.; Jahanmardi, R.; Nouranian, S.; Arjmand, M.; Khonakdar, H.A. Degradation of Polymer Nanocomposites Filled with Graphene Oxide and Reduced Graphene Oxide Nanoparticles: A Review of Current Status. *Polym. Degrad. Stab.* **2022**, *206*, 110179. [CrossRef]
129. Li, J.; Han, M.; Muhammad, Y.; Liu, Y.; Yang, S.; Duan, S.; Huang, W.; Zhao, Z. Comparative Analysis, Road Performance and Mechanism of Modification of Polystyrene Graphene Nanoplatelets (PS-GNPs) and Octadecyl Amine Graphene Nanoplatelets (ODA-GNPs) Modified SBS Incorporated Asphalt Binders. *Constr. Build. Mater.* **2018**, *193*, 501–517. [CrossRef]
130. Wu, S.; Xu, W.; Zhang, F.; Wu, H. Effect of Polyurethane on High- and Low-Temperature Performance of Graphene Oxide-Modified Asphalt and Analysis of the Mechanism Based on Infrared Spectrum. *Coatings* **2022**, *12*, 590. [CrossRef]
131. Wu, F.; Xu, W.; Zhang, F.; Wu, H. Grey Correlation Analysis of Physical Properties and Evaluation Index of Graphene-Oxide-Modified Asphalt. *Coatings* **2022**, *12*, 770. [CrossRef]
132. Zhu, J.; Zhang, K.; Liu, K.; Shi, X. Adhesion Characteristics of Graphene Oxide Modified Asphalt Unveiled by Surface Free Energy and AFM-Scanned Micro-Morphology. *Constr. Build. Mater.* **2021**, *244*, 118404. [CrossRef]
133. Jing, F.; Wang, R.; Zhao, R.; Li, C.; Cai, J.; Ding, G.; Wang, Q.; Xie, H. Enhancement of Bonding and Mechanical Performance of Epoxy Asphalt Bond Coats with Graphene Nanoplatelets. *Polymers* **2023**, *15*, 412. [CrossRef]
134. Malik, S.B.; Saggu, J.I.; Gul, A.; Abbasi, B.A.; Iqbal, J.; Waris, S.; Jardan, Y.A.B.; Chalgham, W. Synthesis and Characterization of Silver and Graphene Nanocomposites and Their Antimicrobial and Photocatalytic Potentials. *Molecules* **2022**, *27*, 5184. [CrossRef] [PubMed]
135. Leone, C.; Di Siena, M.; Genna, S.; Martone, A. Effect of Graphite Nanoplatelets Percentage on the in Plane Thermal Diffusivity of Ultra-Thin Graphene Based (Nanostructured) Composite. *Opt. Laser Technol.* **2022**, *146*, 107552. [CrossRef]
136. Zotti, A.; Zuppolini, S.; Borriello, A.; Zarrelli, M. Polymer Nanocomposites Based on Graphite Nanoplatelets and Amphiphilic Graphene Platelets. *Compos. Part B Eng.* **2022**, *246*, 110223. [CrossRef]
137. Hafeez, M.; Ahmad, N.; Kamal, M.A.; Rafi, J.; ul Haq, M.F.; Jamal; Zaidi, S.B.A.; Nasir, M.A. Experimental Investigation into the Structural and Functional Performance of Graphene Nano-Platelet (GNP)-Doped Asphalt. *Appl. Sci.* **2019**, *9*, 686. [CrossRef]
138. Yang, B.; Pan, Y.; Yu, Y.; Wu, J.; Xia, R.; Wang, S.; Wang, Y.; Su, L.; Miao, J.; Qian, J.; et al. Filler Network Structure in Graphene Nanoplatelet (GNP)-Filled Polymethyl Methacrylate (PMMA) Composites: From Thermorheology to Electrically and Thermally Conductive Properties. *Polym. Test.* **2020**, *89*, 106575. [CrossRef]
139. Clausi, M.; Grasselli, S.; Malchiodi, A.; Bayer, I.S. Thermally Conductive PVDF-Graphene Nanoplatelet (GnP) Coatings. *Appl. Surf. Sci.* **2020**, *529*, 147070. [CrossRef]
140. Liu, L.; Li, Y.; Zhang, H.; Cheng, X.; Fan, Q.; Mu, X. Reaction Kinetics of Three-Dimensional Interface in Graphene Nanoplatelets Reinforced Titanium (GNPs/Ti) Composites as Revealed by in Situ TEM Heating Experiments. *Compos. Part B Eng.* **2022**, *247*, 110237. [CrossRef]
141. Patil, A.; Kiran Kumar Yadav Nartu, M.S.; Ozdemir, F.; Banerjee, R.; Gupta, R.K.; Borkar, T. Enhancement of the Mechanical Properties of Graphene Nanoplatelet (GNP) Reinforced Nickel Matrix Nanocomposites. *Mater. Sci. Eng. A* **2021**, *817*, 141324. [CrossRef]
142. Vallejo, J.P.; Mercatelli, L.; Martina, M.R.; Di Rosa, D.; Dell'Oro, A.; Lugo, L.; Sani, E. Comparative Study of Different Functionalized Graphene-Nanoplatelet Aqueous Nanofluids for Solar Energy Applications. *Renew. Energy* **2019**, *141*, 791–801. [CrossRef]
143. Sandhya, M.; Ramasamy, D.; Kadirgama, K.; Harun, W.S.W.; Saidur, R. Experimental Study on Properties of Hybrid Stable & Surfactant-Free Nanofluids GNPs/CNCs (Graphene Nanoplatelets/Cellulose Nanocrystal) in Water/Ethylene Glycol Mixture for Heat Transfer Application. *J. Mol. Liq.* **2022**, *348*, 118019. [CrossRef]
144. Ambreen, T.; Saleem, A.; Tanveer, M.; Anirudh, K.; Shehzad, S.A.; Park, C.W. Irreversibility and Hydrothermal Analysis of the MWCNTs/GNPs-Based Nanofluids for Electronics Cooling Applications of the Pin-Fin Heat Sinks: Multiphase Eulerian-Lagrangian Modeling. *Case Stud. Therm. Eng.* **2022**, *31*, 101806. [CrossRef]

145. Wang, Y.-Y.; Tan, Y.-Q.; Liu, K.; Xu, H.-N. Preparation and Electrical Properties of Conductive Asphalt Concretes Containing Graphene and Carbon Fibers. *Constr. Build. Mater.* **2022**, *318*, 125875. [CrossRef]
146. Zhang, K.; Gao, X.; Zhang, Q.; Li, T.; Chen, H.; Chen, X. Preparation and Microwave Absorption Properties of Asphalt Carbon Coated Reduced Graphene Oxide/Magnetic CoFe2O4 Hollow Particles Modified Multi-Wall Carbon Nanotube Composites. *J. Alloys Compd.* **2017**, *723*, 912–921. [CrossRef]
147. Yu, R.; Wang, Q.; Wang, W.; Xiao, Y.; Wang, Z.; Zhou, X.; Zhang, X.; Zhu, X.; Fang, C. Polyurethane/Graphene Oxide Nanocomposite and Its Modified Asphalt Binder: Preparation, Properties and Molecular Dynamics Simulation. *Mater. Des.* **2021**, *209*, 109994. [CrossRef]
148. Fernández, S.; Mercado, A.; Cuara, E.; Yeverino-Miranda, C.; Sierra, U. Asphalt as Raw Material of Graphene-like Resources. *Fuel* **2019**, *241*, 297–303. [CrossRef]
149. An, J.; Wang, S.; Huang, M.; Zhang, J.; Wang, P. Removal of Water-Soluble Lignin Model Pollutants with Graphene Oxide Loaded Ironic Sulfide as an Efficient Adsorbent and Heterogeneous Fenton Catalyst. *Arab. J. Chem.* **2022**, *15*, 104338. [CrossRef]
150. Manabe, S.; Adavan Kiliyankil, V.; Takiguchi, S.; Kumashiro, T.; Fugetsu, B.; Sakata, I. Graphene Nanosheets Homogeneously Incorporated in Polyurethane Sponge for the Elimination of Water-Soluble Organic Dyes. *J. Colloid Interface Sci.* **2021**, *584*, 816–826. [CrossRef] [PubMed]
151. Zhang, X.-R.; Guo, J.-G.; Zhou, L.-J. Experimental and Theoretical Investigation on the Adsorption Properties of Benzene on Graphene Surface: Influence of PH and Edge Effects. *Chem. Eng. J.* **2022**, *440*, 135794. [CrossRef]
152. Bhattacharyya, S.; Poi, R.; Baskey Sen, M.; Mandal, S.; Hazra, D.K.; Karmakar, R. Efficient Fabrication of PH-Modified Graphene Nano-Adsorbent for Effective Determination and Monitoring of Multi-Class Pesticide Residues in Market-Fresh Vegetables by GC-MS. *J. Food Compos. Anal.* **2023**, *118*, 105153. [CrossRef]
153. Chen, Q.; Wang, C.; Qiao, Z.; Guo, T. Graphene/Tourmaline Composites as a Filler of Hot Mix Asphalt Mixture: Preparation and Properties. *Constr. Build. Mater.* **2020**, *239*, 117859. [CrossRef]
154. Pavlov, S.V.; Kozhevnikova, E.O.; Kislenko, S.A. Effect of the Number of Graphene Layers on the Electron Transfer Kinetics at Metal/Graphene Heterostructures. *J. Electroanal. Chem.* **2022**, *925*, 116895. [CrossRef]
155. Liu, J.; Hao, P.; Jiang, W.; Sun, B. Rheological Properties of SBS Modified Asphalt Incorporated Polyvinylpyrrolidone Stabilized Graphene Nanoplatelets. *Constr. Build. Mater.* **2021**, *298*, 123850. [CrossRef]
156. Qi, G.; Wang, Q.; Zhang, R.; Guo, Z.; Zhan, D.; Liu, S. Effect of RGO/GNP on the Electrical Conductivity and Piezoresistance of Cement-Based Composite Subjected to Dynamic Loading. *Constr. Build. Mater.* **2023**, *368*, 130340. [CrossRef]
157. Ripoll, L.; Legnaioli, S.; Palleschi, V.; Hidalgo, M. Evaluation of Electrosprayed Graphene Oxide Coatings for Elemental Analysis by Thin Film Microextraction Followed by Laser-Induced Breakdown Spectroscopy Detection. *Spectrochim. Acta Part B At. Spectrosc.* **2021**, *183*, 106267. [CrossRef]
158. Li, X.; Wang, Y.-M.; Wu, Y.-L.; Wang, H.-R.; Chen, M.; Sun, H.-D.; Fan, L. Properties and Modification Mechanism of Asphalt with Graphene as Modifier. *Constr. Build. Mater.* **2021**, *272*, 121919. [CrossRef]
159. Zhu, J.; Zhang, K.; Liu, K.; Shi, X. Performance of Hot and Warm Mix Asphalt Mixtures Enhanced by Nano-Sized Graphene Oxide. *Constr. Build. Mater.* **2019**, *217*, 273–282. [CrossRef]
160. Moretti, L.; Fabrizi, N.; Fiore, N.; D'Andrea, A. Mechanical Characteristics of Graphene Nanoplatelets-Modified Asphalt Mixes: A Comparison with Polymer- and Not-Modified Asphalt Mixes. *Materials* **2021**, *14*, 2434. [CrossRef]
161. Wang, R.; Qi, Z.; Li, R.; Yue, J. Investigation of the Effect of Aging on the Thermodynamic Parameters and the Intrinsic Healing Capability of Graphene Oxide Modified Asphalt Binders. *Constr. Build. Mater.* **2020**, *230*, 116984. [CrossRef]
162. Nciri, N.; Kim, N.; Cho, N. Spent Graphite from End-of-Life Lithium-Ion Batteries (LIBs) as a Promising Nanoadditive to Boost Road Pavemen Performance. *Materials* **2021**, *14*, 7908. [CrossRef]
163. Zhang, X.; He, J.-X.; Huang, G.; Zhou, C.; Feng, M.-M.; Li, Y. Preparation and Characteristics of Ethylene Bis(Stearamide)-Based Graphene-Modified Asphalt. *Materials* **2019**, *12*, 757. [CrossRef] [PubMed]
164. Huang, H.-D.; Ren, P.-G.; Xu, J.-Z.; Xu, L.; Zhong, G.-J.; Hsiao, B.S.; Li, Z.-M. Improved Barrier Properties of Poly(Lactic Acid) with Randomly Dispersed Graphene Oxide Nanosheets. *J. Memb. Sci.* **2014**, *464*, 110–118. [CrossRef]
165. Wang, L.; Shen, A.; Wang, W.; Yang, J.; He, Z.; Zhijie, T. Graphene/Nickel/Carbon Fiber Composite Conductive Asphalt: Optimization, Electrical Properties and Heating Performance. *Case Stud. Constr. Mater.* **2022**, *17*, e01402. [CrossRef]
166. Wu, H.; Shen, A.; Pan, H.; Hou, X.; Yu, P.; Li, Y. Mechanism of Multilayer Graphene Nanoplatelets and Its Effects on the Rheological Properties and Thermal Stability of Styrene-Butadiene-Styrene Modified Asphalt. *Diam. Relat. Mater.* **2022**, *130*, 109434. [CrossRef]
167. Liu, J.; Hao, P.; Dou, Z.; Wang, J.; Ma, L. Rheological, Healing and Microstructural Properties of Unmodified and Crumb Rubber Modified Asphalt Incorporated with Graphene/Carbon Black Composite. *Constr. Build. Mater.* **2021**, *305*, 124512. [CrossRef]
168. Huang, J.; Liu, Y.; Subhan, S.; Quan, X.; Zhong, H.; Li, J.; Zhao, Z. Fast Deposition of Fe3+ Chelated Tannic Acid Network via Salt Induction over Graphene Oxide Based SBS Modified Asphalt. *Constr. Build. Mater.* **2021**, *307*, 125009. [CrossRef]
169. D'angelo, S.; Ferrotti, G.; Cardone, F.; Canestrari, F. Asphalt Binder Modification with Plastomeric Compounds Containing Recycled Plastics and Graphene. *Materials* **2022**, *15*, 516. [CrossRef]
170. Cheng, I.F.; Xie, Y.; Allen Gonzales, R.; Brejna, P.R.; Sundararajan, J.P.; Fouetio Kengne, B.A.; Eric Aston, D.; McIlroy, D.N.; Foutch, J.D.; Griffiths, P.R. Synthesis of Graphene Paper from Pyrolyzed Asphalt. *Carbon N. Y.* **2011**, *49*, 2852–2861. [CrossRef]

171. Singh, B.B.; Mohanty, F.; Das, S.S.; Swain, S.K. Graphene Sandwiched Crumb Rubber Dispersed Hot Mix Asphalt. *J. Traffic Transp. Eng.* **2020**, *7*, 652–667. [CrossRef]
172. Li, Z.; Guo, T.; Chen, Y.; Dong, L.; Chen, Q.; Hao, M.; Zhao, X.; Liu, J. Study on Rheological Properties of Graphene Oxide/Rubber Crowd Composite-Modified Asphalt. *Materials* **2022**, *15*, 6185. [CrossRef]
173. Zhang, H.; Yu, J.; Wu, S. Effect of Montmorillonite Organic Modification on Ultraviolet Aging Properties of SBS Modified Bitumen. *Constr. Build. Mater.* **2012**, *27*, 553–559. [CrossRef]
174. Joshi, J.; Homburg, S.V.; Ehrmann, A. Atomic Force Microscopy (AFM) on Biopolymers and Hydrogels for Biotechnological Applications—Possibilities and Limits. *Polymers* **2022**, *14*, 1267. [CrossRef] [PubMed]
175. Peng, C.; Guo, C.; You, Z.; Xu, F.; Ma, W.; You, L.; Li, T.; Zhou, L.; Huang, S.; Ma, H.; et al. The Effect of Waste Engine Oil and Waste Polyethylene on UV Aging Resistance of Asphalt. *Polymers* **2020**, *12*, 602. [CrossRef]
176. Demir-Yilmaz, I.; Guiraud, P.; Formosa-Dague, C. The Contribution of Atomic Force Microscopy (AFM) in Microalgae Studies: A Review. *Algal Res.* **2021**, *60*, 102506. [CrossRef]
177. Johnson, D.; Hilal, N.; Bowen, W.R. Chapter 1: Basic Principles of Atomic Force Microscopy. In *Atomic Force Microscopy in Process Engineering: Introduction to AFM for Improved Processes and Products*; Elsevier: Amsterdam, The Netherlands, 2009; pp. 1–30.
178. Dorobantu, L.S.; Goss, G.G.; Burrell, R.E. Atomic Force Microscopy: A Nanoscopic View of Microbial Cell Surfaces. *Micron* **2012**, *43*, 1312–1322. [CrossRef]
179. Luís, A.T.; Hlúbiková, D.; Vaché, V.; Choquet, P.; Hoffmann, L.; Ector, L. Atomic Force Microscopy (AFM) Application to Diatom Study: Review and Perspectives. *J. Appl. Phycol.* **2017**, *29*, 2989–3001. [CrossRef]
180. Das, P.K.; Kringos, N.; Birgisson, B. Microscale Investigation of Thin Film Surface Ageing of Bitumen. *J. Microsc.* **2014**, *254*, 95–107. [CrossRef]
181. Zhang, H.L.; Yu, J.Y.; Feng, Z.G.; Xue, L.H.; Wu, S.P. Effect of Aging on the Morphology of Bitumen by Atomic Force Microscopy. *J. Microsc.* **2012**, *246*, 11–19. [CrossRef]
182. Blom, J.; Soenen, H.; Van den Brande, N.; Van den bergh, W. New Evidence on the Origin of 'Bee Structures' on Bitumen and Oils, by Atomic Force Microscopy (AFM) and Confocal Laser Scanning Microscopy (CLSM). *Fuel* **2021**, *303*, 121265. [CrossRef]
183. Pipintakos, G.; Hasheminejad, N.; Lommaert, C.; Bocharova, A.; Blom, J. Application of Atomic Force (AFM), Environmental Scanning Electron (ESEM) and Confocal Laser Scanning Microscopy (CLSM) in Bitumen: A Review of the Ageing Effect. *Micron* **2021**, *147*, 103083. [CrossRef]
184. Hung, A.M.; Kazembeyki, M.; Hoover, C.G.; Fini, E.H. Evolution of Morphological and Nanomechanical Properties of Bitumen Thin Films as a Result of Compositional Changes Due to Ultraviolet Radiation. *ACS Sustain. Chem. Eng.* **2019**, *7*, 18005–18014. [CrossRef]
185. Abdelaziz, A.; Epps Martin, A.; Masad, E.; Arámbula Mercado, E.; Kaseer, F. Effects of Ageing and Recycling Agents on the Multiscale Properties of Binders with High RAP Contents. *Int. J. Pavement Eng.* **2020**, *23*, 1248–1270. [CrossRef]
186. Motamed, A.; Bhasin, A.; Liechti, K.M. Using the Poker-Chip Test for Determining the Bulk Modulus of Asphalt Binders. *Mech. Time-Dependent Mater.* **2014**, *18*, 197–215. [CrossRef]
187. Kim, Y.S.; Sigwarth, T.; Büchner, J.; Wistuba, M.P. Accelerated Dynamic Shear Rheometer Fatigue Test for Investigating Asphalt Mastic. *Road Mater. Pavement Des.* **2021**, *22*, S383–S396. [CrossRef]
188. Wu, J.; Wang, H.; Liu, Q.; Gao, Y.; Liu, S. A Temperature-Independent Methodology for Polymer Bitumen Modification Evaluation Based on DSR Measurement. *Polymers* **2022**, *14*, 848. [CrossRef]
189. Hintz, C.; Bahia, H. Understanding Mechanisms Leading to Asphalt Binder Fatigue in the Dynamic Shear Rheometer. *Road Mater. Pavement Des.* **2013**, *14*, 231–251. [CrossRef]
190. Ge, D.; Chen, S.; You, Z.; Yang, X.; Yao, H.; Ye, M.; Yap, Y.K. Correlation of DSR Results and FTIR's Carbonyl and Sulfoxide Indexes: Effect of Aging Temperature on Asphalt Rheology. *J. Mater. Civ. Eng.* **2019**, *31*, 04019115. [CrossRef]
191. Kim, Y.J.; Cho, B.; Lee, S.-J.; Hu, J.; Wilde, J.W. Investigation of Rheological Properties of Blended Cement Pastes Using Rotational Viscometer and Dynamic Shear Rheometer. *Adv. Mater. Sci. Eng.* **2018**, *2018*, 1–6. [CrossRef]
192. Chen, Z.; Zhang, H.; Shi, C.; Wei, C. Rheological Performance Investigation and Sustainability Evaluation of Asphalt Binder with Thermochromic Powders under Solar Radiation. *Sol. Energy Mater. Sol. Cells* **2019**, *191*, 175–182. [CrossRef]
193. Zhang, H.; Chen, Z.; Xu, G.; Shi, C. Evaluation of Aging Behaviors of Asphalt Binders through Different Rheological Indices. *Fuel* **2018**, *221*, 78–88. [CrossRef]
194. Walubita, L.F.; Gonzalez-Hernandez, J.G.; Martinez-Arguelles, G.; Tanvir, H.; Fuentes, L.; Tahami, S.A. Statistical Evaluation of the Material-Source Effects on the DSR Rheological Properties of Plant-Mix Extracted Asphalt-Binders. *Materials* **2021**, *14*, 1931. [CrossRef] [PubMed]
195. Tulej, M.; Iakovleva, M.; Leya, I.; Wurz, P. A Miniature Mass Analyser for In-Situ Elemental Analysis of Planetary Material-Performance Studies. *Anal. Bioanal. Chem.* **2011**, *399*, 2185–2200. [CrossRef] [PubMed]
196. Canizo, B.V.; Escudero, L.B.; Pérez, M.B.; Pellerano, R.G.; Wuilloud, R.G. Intra-Regional Classification of Grape Seeds Produced in Mendoza Province (Argentina) by Multi-Elemental Analysis and Chemometrics Tools. *Food Chem.* **2018**, *242*, 272–278. [CrossRef] [PubMed]
197. Kanngießer, B.; Malzer, W.; Mantouvalou, I.; Sokaras, D.; Karydas, A.G. A Deep View in Cultural Heritage-Confocal Micro X-ray Spectroscopy for Depth Resolved Elemental Analysis. *Appl. Phys. A Mater. Sci. Process.* **2012**, *106*, 325–338. [CrossRef]

198. Aguirre, M.A.; Legnaioli, S.; Almodóvar, F.; Hidalgo, M.; Palleschi, V.; Canals, A. Elemental Analysis by Surface-Enhanced Laser-Induced Breakdown Spectroscopy Combined with Liquid-Liquid Microextraction. *Spectrochim. Acta Part B* **2013**, *79–80*, 88–93. [CrossRef]
199. Ruiz, F.J.; Ripoll, L.; Hidalgo, M.; Canals, A. Dispersive Micro Solid-Phase Extraction (DμSPE) with Graphene Oxide as Adsorbent for Sensitive Elemental Analysis of Aqueous Samples by Laser Induced Breakdown Spectroscopy (LIBS). *Talanta* **2019**, *191*, 162–170. [CrossRef]
200. Kaiser, J.; Novotný, K.; Martin, M.Z.; Hrdlička, A.; Malina, R.; Hartl, M.; Adam, V.; Kizek, R. Trace Elemental Analysis by Laser-Induced Breakdown Spectroscopy—Biological Applications. *Surf. Sci. Rep.* **2012**, *67*, 233–243. [CrossRef]
201. Buddhachat, K.; Klinhom, S.; Siengdee, P.; Brown, J.L.; Nomsiri, R.; Kaewmong, P.; Thitaram, C.; Mahakkanukrauh, P.; Nganvongpanit, K. Elemental Analysis of Bone, Teeth, Horn and Antler in Different Animal Species Using Non- Invasive Handheld X-ray Fluorescence. *PLoS ONE* **2016**, *11*, e0155458. [CrossRef]
202. Alshehabi, A.; Sasaki, N.; Kawai, J. Total Reflection X-ray Photoelectron Spectroscopy as a Semiconductor Lubricant Elemental Analysis Method. *Spectrochim. Acta Part B* **2015**, *114*, 34–37. [CrossRef]
203. Cao, Z.; Xue, L.; Wu, M.; He, B.; Yu, J.; Chen, M. Effect of Etched Layered Double Hydroxides on Anti Ultraviolet Aging Properties of Bitumen. *Constr. Build. Mater.* **2018**, *178*, 42–50. [CrossRef]
204. He, X.; Hochstein, D.; Ge, Q.; Ali, A.W.; Chen, F.; Yin, H. Accelerated Aging of Asphalt by UV Photo-Oxidation Considering Moisture and Condensation Effects. *J. Mater. Civ. Eng.* **2018**, *30*, 04017261. [CrossRef]
205. Greczynski, G.; Hultman, L.; Odén, M. X-ray Photoelectron Spectroscopy Studies of Ti1-XAlxN ($0 \leq x \leq 0.83$) High-Temperature Oxidation: The Crucial Role of Al Concentration. *Surf. Coatings Technol.* **2019**, *374*, 923–934. [CrossRef]
206. Kohzadi, H.; Soleiman-Beigi, M. XPS and Structural Studies of Fe3O4-PTMS-NAS@Cu as a Novel Magnetic Natural Asphalt Base Network and Recoverable Nanocatalyst for the Synthesis of Biaryl Compounds. *Sci. Rep.* **2021**, *11*, 24508. [CrossRef] [PubMed]
207. Patel, M.; Azanza Ricardo, C.L.; Scardi, P.; Aswath, P.B. Morphology, Structure and Chemistry of Extracted Diesel Soot—Part I: Transmission Electron Microscopy, Raman Spectroscopy, X-ray Photoelectron Spectroscopy and Synchrotron X-ray Diffraction Study. *Tribol. Int.* **2012**, *52*, 29–39. [CrossRef]
208. Aluha, J.; Blais, S.; Abatzoglou, N. Phase Quantification of Carbon Support by X-ray Photoelectron Spectroscopy (XPS) in Plasma-Synthesized Fischer–Tropsch Nanocatalysts. *Catal. Letters* **2018**, *148*, 2149–2161. [CrossRef]
209. Chinchón-Payá, S.; Aguado, A.; Coloma, F.; Chinchón, S. Study of Aggregate Samples with Iron Sulfides through Micro X-ray Fluorescence (MXRF) and X-ray Photoelectron Spectroscopy (XPS). *Mater. Struct.* **2015**, *48*, 1285–1290. [CrossRef]
210. Lefebvre, J.; Galli, F.; Bianchi, C.L.; Patience, G.S.; Boffito, D.C. Experimental Methods in Chemical Engineering: X-ray Photoelectron Spectroscopy-XPS. *Can. J. Chem. Eng.* **2019**, *97*, 2588–2593. [CrossRef]
211. Zhang, X.; Han, C.; Zhou, X.; Otto, F.; Zhang, F. Characterizing the Diffusion and Rheological Properties of Aged Asphalt Binder Rejuvenated with Bio-Oil Based on Molecular Dynamic Simulations and Laboratory Experimentations. *Molecules* **2021**, *26*, 7080. [CrossRef]
212. Petersen, J.C. *Chapter 14: Chemical Composition of Asphalt as Related to Asphalt Durability*; Elsevier: Amsterdam, The Netherlands, 2000; Volume 40.
213. Li, Y.; Wu, S.; Liu, Q.; Dai, Y.; Li, C.; Li, H.; Nie, S.; Song, W. Aging Degradation of Asphalt Binder by Narrow-Band UV Radiations with a Range of Dominant Wavelengths. *Constr. Build. Mater.* **2019**, *220*, 637–650. [CrossRef]
214. Li, Y.; Chen, Q.; Xu, K.; Kaneko, T.; Hatakeyama, R. Synthesis of Graphene Nanosheets from Petroleum Asphalt by Pulsed Arc Discharge in Water. *Chem. Eng. J.* **2013**, *215–216*, 45–49. [CrossRef]
215. Sreeprasad, T.S.; Sen Gupta, S.; Maliyekkal, S.M.; Pradeep, T. Immobilized Graphene-Based Composite from Asphalt: Facile Synthesis and Application in Water Purification. *J. Hazard. Mater.* **2013**, *246–247*, 213–220. [CrossRef] [PubMed]
216. Porot, L.; Mouillet, V.; Margaritis, A.; Haghshenas, H.; Elwardany, M.; Apostolidis, P. Fourier-Transform Infrared Analysis and Interpretation for Bituminous Binders. *Road Mater. Pavement Des.* **2022**, *24*, 462–483. [CrossRef]
217. Feng, Z.G.; Wang, S.J.; Bian, H.J.; Guo, Q.L.; Li, X.J. FTIR and Rheology Analysis of Aging on Different Ultraviolet Absorber Modified Bitumens. *Constr. Build. Mater.* **2016**, *115*, 48–53. [CrossRef]
218. Feng, Z.; Cai, F.; Yao, D.; Li, X. Aging Properties of Ultraviolet Absorber/SBS Modified Bitumen Based on FTIR Analysis. *Constr. Build. Mater.* **2021**, *273*, 121713. [CrossRef]
219. Yu, H.; Bai, X.; Qian, G.; Wei, H.; Gong, X.; Jin, J.; Li, Z. Impact of Ultraviolet Radiation on the Aging Properties of SBS-Modified Asphalt Binders. *Polymers* **2019**, *11*, 1111. [CrossRef]
220. Xu, S.; Dang, L.; Yu, J.; Xue, L.; Hu, C.; Que, Y. Evaluation of Ultraviolet Aging Resistance of Bitumen Containing Different Organic Layered Double Hydroxides. *Constr. Build. Mater.* **2018**, *192*, 696–703. [CrossRef]
221. Liu, K.; Zhang, K.; Wu, J.; Muhunthan, B.; Shi, X. Evaluation of Mechanical Performance and Modification Mechanism of Asphalt Modified with Graphene Oxide and Warm Mix Additives. *J. Clean. Prod.* **2018**, *193*, 87–96. [CrossRef]
222. Xie, X.; Tong, S.; Ding, Y.; Liu, H.; Liang, L. Effect of the Amount of Mineral Powder on the Ultraviolet Aging Properties of Asphalt. *Adv. Mater. Sci. Eng.* **2016**, *2016*, 5207391. [CrossRef]
223. Zhou, X.; Zhao, G.; Wu, S.; Tighe, S.; Pickel, D.; Chen, M.; Adhikari, S.; Gao, Y. Effects of Biochar on the Chemical Changes and Phase Separation of Bio-Asphalt under Different Aging Conditions. *J. Clean. Prod.* **2020**, *263*, 121532. [CrossRef]
224. Zhan, Y.; Xie, J.; Wu, Y.; Wang, Y. Synergetic Effect of Nano-ZnO and Trinidad Lake Asphalt for Antiaging Properties of SBS-Modified Asphalt. *Adv. Civ. Eng.* **2020**, *2020*, 3239793. [CrossRef]

225. Zadshir, M.; Hosseinnezhad, S.; Ortega, R.; Chen, F.; Hochstein, D.; Xie, J.; Yin, H.; Parast, M.M.; Fini, E.H. Application of a Biomodifier as Fog Sealants to Delay Ultraviolet Aging of Bituminous Materials. *J. Mater. Civ. Eng.* **2018**, *30*, 04018310. [CrossRef]
226. Li, Y.; Wu, S.; Dai, Y.; Pang, L.; Liu, Q.; Xie, J.; Kong, D. Investigation of Sodium Stearate Organically Modified LDHs Effect on the Anti Aging Properties of Asphalt Binder. *Constr. Build. Mater.* **2018**, *172*, 509–518. [CrossRef]
227. Li, Y.; Wu, S.; Liu, Q.; Nie, S.; Li, H.; Dai, Y.; Pang, L.; Li, C.; Zhang, A. Field Evaluation of LDHs Effect on the Aging Resistance of Asphalt Concrete after Four Years of Road Service. *Constr. Build. Mater.* **2019**, *208*, 192–203. [CrossRef]
228. Zeng, W.; Wu, S.; Wen, J.; Chen, Z. The Temperature Effects in Aging Index of Asphalt during UV Aging Process. *Constr. Build. Mater.* **2015**, *93*, 1125–1131. [CrossRef]
229. Wu, S.; Pang, L.; Liu, G.; Zhu, J. Laboratory Study on Ultraviolet Radiation Aging of Bitumen. *J. Mater. Civ. Eng.* **2010**, *22*, 767–772. [CrossRef]
230. Markin, A.V.; Arzhanukhina, A.I.; Markina, N.E.; Goryacheva, I.Y. Analytical Performance of Electrochemical Surface-Enhanced Raman Spectroscopy: A Critical Review. *Trends Anal. Chem.* **2022**, *157*, 116776. [CrossRef]
231. Hemati Farsani, M.; Darbani, S.M.R.; Mobashery, A. Application of Deep Raman Spectroscopy to Detect Ammonium Nitrate Concealed in Color Fabrics. *Vib. Spectrosc.* **2022**, *121*, 103405. [CrossRef]
232. Fernández-Manteca, M.G.; Ocampo-Sosa, A.A.; Ruiz de Alegría-Puig, C.; Pía Roiz, M.; Rodríguez-Grande, J.; Madrazo, F.; Calvo, J.; Rodríguez-Cobo, L.; López-Higuera, J.M.; Fariñas, M.C.; et al. Automatic Classification of Candida Species Using Raman Spectroscopy and Machine Learning. *Spectrochim. Acta—Part A Mol. Biomol. Spectrosc.* **2023**, *290*, 122270. [CrossRef]
233. Ma, L.; Qiu, W.; Fan, X. Stress/Strain Characterization in Electronic Packaging by Micro-Raman Spectroscopy: A Review. *Microelectron. Reliab.* **2021**, *118*, 114045. [CrossRef]
234. Sun, Y.; Tang, H.; Zou, X.; Meng, G.; Wu, N. Raman Spectroscopy for Food Quality Assurance and Safety Monitoring: A Review. *Curr. Opin. Food Sci.* **2022**, *47*, 100910. [CrossRef]
235. Estefany, C.; Sun, Z.; Hong, Z.; Du, J. Raman Spectroscopy for Profiling Physical and Chemical Properties of Atmospheric Aerosol Particles: A Review. *Ecotoxicol. Environ. Saf.* **2023**, *249*, 114405. [CrossRef] [PubMed]
236. Neo, E.R.K.; Yeo, Z.; Low, J.S.C.; Goodship, V.; Debattista, K. A Review on Chemometric Techniques with Infrared, Raman and Laser-Induced Breakdown Spectroscopy for Sorting Plastic Waste in the Recycling Industry. *Resour. Conserv. Recycl.* **2022**, *180*, 106217. [CrossRef]
237. Zhou, Q.; Xiao, X.; Pan, L.; Tian, H. The Relationship between Micro-Raman Spectral Parameters and Reflectance of Solid Bitumen. *Int. J. Coal Geol.* **2014**, *121*, 19–25. [CrossRef]
238. Nciri, N.; Kim, J.; Kim, N.; Cho, N. An In-Depth Investigation into the Physicochemical, Thermal, Microstructural, and Rheological Properties of Petroleum and Natural Asphalts. *Materials* **2016**, *9*, 859. [CrossRef]
239. Gulisano, F.; Buasiri, T.; Apaza Apaza, F.R.; Cwirzen, A.; Gallego, J. Piezoresistive Behavior of Electric Arc Furnace Slag and Graphene Nanoplatelets Asphalt Mixtures for Self-Sensing Pavements. *Autom. Constr.* **2022**, *142*, 104534. [CrossRef]
240. Caputo, P.; Porto, M.; Angelico, R.; Loise, V.; Calandra, P.; Oliviero Rossi, C. Bitumen and Asphalt Concrete Modified by Nanometer-Sized Particles: Basic Concepts, the State of the Art and Future Perspectives of the Nanoscale Approach. *Adv. Colloid Interface Sci.* **2020**, *285*, 102283. [CrossRef]
241. Liu, Z.; Tu, Z.; Li, Y.; Yang, F.; Han, S.; Yang, W.; Zhang, L.; Wang, G.; Xu, C.; Gao, J. Synthesis of Three-Dimensional Graphene from Petroleum Asphalt by Chemical Vapor Deposition. *Mater. Lett.* **2014**, *122*, 285–288. [CrossRef]
242. Zhang, K.; Gao, X.; Zhang, Q.; Li, T.; Chen, H.; Chen, X. Synthesis, Characterization and Electromagnetic Wave Absorption Properties of Asphalt Carbon Coated Graphene/Magnetic NiFe2O4 Modified Multi-Wall Carbon Nanotube Composites. *J. Alloys Compd.* **2017**, *721*, 268–275. [CrossRef]
243. Xie, Y.; McAllister, S.D.; Hyde, S.A.; Sundararajan, J.P.; FouetioKengne, B.A.; McIlroy, D.N.; Cheng, I.F. Sulfur as an Important Co-Factor in the Formation of Multilayer Graphene in the Thermolyzed Asphalt Reaction. *J. Mater. Chem.* **2012**, *22*, 5723–5729. [CrossRef]
244. Vos, K.; Vandenberghe, N.; Elsen, J. Surface Textural Analysis of Quartz Grains by Scanning Electron Microscopy (SEM): From Sample Preparation to Environmental Interpretation. *Earth-Science Rev.* **2014**, *128*, 93–104. [CrossRef]
245. Iwata, H.; Hayashi, Y.; Hasegawa, A.; Terayama, K.; Okuno, Y. Classification of Scanning Electron Microscope Images of Pharmaceutical Excipients Using Deep Convolutional Neural Networks with Transfer Learning. *Int. J. Pharm. X* **2022**, *4*, 100135. [CrossRef] [PubMed]
246. Mokhtari, A.; Lee, H.D.; Williams, R.C.; Guymon, C.A.; Scholte, J.P.; Schram, S. A Novel Approach to Evaluate Fracture Surfaces of Aged and Rejuvenator-Restored Asphalt Using Cryo-SEM and Image Analysis Techniques. *Constr. Build. Mater.* **2017**, *133*, 301–313. [CrossRef]
247. López de la Rosa, F.; Sánchez-Reolid, R.; Gómez-Sirvent, J.L.; Morales, R.; Fernández-Caballero, A. A Review on Machine and Deep Learning for Semiconductor Defect Classification in Scanning Electron Microscope Images. *Appl. Sci.* **2021**, *11*, 9508. [CrossRef]
248. Luo, Q. Electron Microscopy and Spectroscopy in the Analysis of Friction and Wear Mechanisms. *Lubricants* **2018**, *6*, 58. [CrossRef]
249. Mazumder, M.; Ahmed, R.; Wajahat Ali, A.; Lee, S.-J. SEM and ESEM Techniques Used for Analysis of Asphalt Binder and Mixture: A State of the Art Review. *Constr. Build. Mater.* **2018**, *186*, 313–329. [CrossRef]
250. Bangaru, S.S.; Wang, C.; Zhou, X.; Hassan, M. Scanning Electron Microscopy (SEM) Image Segmentation for Microstructure Analysis of Concrete Using U-Net Convolutional Neural Network. *Autom. Constr.* **2022**, *144*, 104602. [CrossRef]

251. Mahltig, B.; Grethe, T. High-Performance and Functional Fiber Materials—A Review of Properties, Scanning Electron Microscopy SEM and Electron Dispersive Spectroscopy EDS. *Textiles* **2022**, *2*, 209–251. [CrossRef]
252. Naskar, M.; Reddy, K.S.; Chaki, T.K.; Divya, M.K.; Deshpande, A.P. Effect of Ageing on Different Modified Bituminous Binders: Comparison between RTFOT and Radiation Ageing. *Mater. Struct.* **2013**, *46*, 1227–1241. [CrossRef]
253. Sun, X.; Yuan, J.; Liu, Z.; Qin, X.; Yin, Y. Evaluation and Characterization on the Segregation and Dispersion of Anti-UV Aging Modifying Agent in Asphalt Binder. *Constr. Build. Mater.* **2021**, *289*, 123204. [CrossRef]
254. Saadatkhah, N.; Carillo Garcia, A.; Ackermann, S.; Leclerc, P.; Latifi, M.; Samih, S.; Patience, G.S.; Chaouki, J. Experimental Methods in Chemical Engineering: Thermogravimetric Analysis—TGA. *Can. J. Chem. Eng.* **2020**, *98*, 34–43. [CrossRef]
255. Bach, Q.-V.; Chen, W.-H. Pyrolysis Characteristics and Kinetics of Microalgae via Thermogravimetric Analysis (TGA): A State-of-the-Art Review. *Bioresour. Technol.* **2017**, *246*, 88–100. [CrossRef] [PubMed]
256. Cai, J.; Xu, D.; Dong, Z.; Yu, X.; Yang, Y.; Banks, S.W.; Bridgwater, A.V. Processing Thermogravimetric Analysis Data for Isoconversional Kinetic Analysis of Lignocellulosic Biomass Pyrolysis: Case Study of Corn Stalk. *Renew. Sustain. Energy Rev.* **2018**, *82*, 2705–2715. [CrossRef]
257. Farivar, F.; Yap, P.L.; Hassan, K.; Tung, T.T.; Tran, D.N.H.; Pollard, A.J.; Losic, D. Unlocking Thermogravimetric Analysis (TGA) in the Fight against "Fake Graphene" Materials. *Carbon N. Y.* **2021**, *179*, 505–513. [CrossRef]
258. Vhathvarothai, N.; Ness, J.; Yu, J. An Investigation of Thermal Behaviour of Biomass and Coal during Co-Combustion Using Thermogravimetric Analysis (TGA). *Int. J. Energy Res.* **2014**, *38*, 804–812. [CrossRef]
259. Evangelopoulos, P.; Kantarelis, E.; Yang, W. Investigation of the Thermal Decomposition of Printed Circuit Boards (PCBs) via Thermogravimetric Analysis (TGA) and Analytical Pyrolysis (Py-GC/MS). *J. Anal. Appl. Pyrolysis* **2015**, *115*, 337–343. [CrossRef]
260. Damartzis, T.; Vamvuka, D.; Sfakiotakis, S.; Zabaniotou, A. Thermal Degradation Studies and Kinetic Modeling of Cardoon (Cynara Cardunculus) Pyrolysis Using Thermogravimetric Analysis (TGA). *Bioresour. Technol.* **2011**, *102*, 6230–6238. [CrossRef] [PubMed]
261. Xu, S.; Yu, J.; Wu, W.; Xue, L.; Sun, Y. Synthesis and Characterization of Layered Double Hydroxides Intercalated by UV Absorbents and Their Application in Improving UV Aging Resistance of Bitumen. *Appl. Clay Sci.* **2015**, *114*, 112–119. [CrossRef]
262. Mansa, R.; Zou, S. Thermogravimetric Analysis of Microplastics: A Mini Review. *Environ. Adv.* **2021**, *5*, 100117. [CrossRef]
263. Clausse, D.; Gomez, F.; Pezron, I.; Komunjer, L.; Dalmazzone, C. Morphology Characterization of Emulsions by Differential Scanning Calorimetry. *Adv. Colloid Interface Sci.* **2005**, *117*, 59–74. [CrossRef]
264. Ahmadi Khoshooei, M.; Fazlollahi, F.; Maham, Y. A Review on the Application of Differential Scanning Calorimetry (DSC) to Petroleum Products: Characterization and Kinetic Study. *J. Therm. Anal. Calorim.* **2019**, *138*, 3455–3484. [CrossRef]
265. Ahmadi Khoshooei, M.; Fazlollahi, F.; Maham, Y.; Hassan, A.; Pereira-Almao, P. A Review on the Application of Differential Scanning Calorimetry (DSC) to Petroleum Products: Wax Crystallization Study and Structural Analysis. *J. Therm. Anal. Calorim.* **2019**, *138*, 3485–3510. [CrossRef]
266. Gill, P.; Moghadam, T.T.; Ranjbar, B. Differential Scanning Calorimetry Techniques: Applications in Biology and Nanoscience. *J. Biomol. Tech.* **2010**, *21*, 167–193.
267. Leyva-Porras, C.; Cruz-Alcantar, P.; Espinosa-Sol, V.; Martinez-Guerra, E.; Piñon-Balderrama, C.I.; Compean-Martinez, I.; Saavedra-Leos, M.Z. Application of Differential Scanning Calorimetry (DSC) and Modulated Differential Scanning Calorimetry (MDSC) in Food and Drug Industries. *Polymers* **2019**, *12*, 5. [CrossRef] [PubMed]
268. Schick, C. Differential Scanning Calorimetry (DSC) of Semicrystalline Polymers. *Anal. Bioanal. Chem.* **2009**, *395*, 1589–1611. [CrossRef] [PubMed]
269. Zeng, S.; Gong, X.; Han, X.; Xu, S.; Xu, J.; Li, X.; Yu, J. Effect of Organic Attapulgite on Properties of SBS Modified Asphalt Waterproofing Membranes. *Constr. Build. Mater.* **2022**, *360*, 129606. [CrossRef]
270. Nciri, N.; Kim, N.; Caron, A. Unlocking the Hidden Potential of Cosmetics Waste for Building Sustainable Green Pavements in the Future: A Case Study of Discarded Lipsticks. *Molecules* **2022**, *27*, 1697. [CrossRef]
271. Akinnifesi, J.O.; Adebiyi, F.M.; Olafisan, K.F. Structural Characterization of Asphaltenes Derived from Nigerian Bitumen Using the X-ray Diffraction Technique. *Pet. Sci. Technol.* **2017**, *35*, 1667–1672. [CrossRef]
272. Siddiqui, M.N.; Ali, M.F.; Shirokoff, J. Use of X-ray Diffraction in Assessing the Aging Pattern of Asphalt Fractions. *Fuel* **2002**, *81*, 51–58. [CrossRef]
273. Ansar, M.; Sikandar, M.A.; Althoey, F.; Tariq, M.A.U.R.; Alyami, S.H.; Elsayed Elkhatib, S. Rheological, Aging, and Microstructural Properties of Polycarbonate and Polytetrafluoroethylene Modified Bitumen. *Polymers* **2022**, *14*, 3283. [CrossRef]
274. Chladil, L.; Cech, O.; Vanýsek, P. XRD Study of Lead Sulfate Crystal Growth in Sulfuric Acid Solution. *ECS Trans.* **2016**, *74*, 147–155. [CrossRef]
275. Grilli, M.L.; Yilmaz, M.; Aydogan, S.; Cirak, B.B. Room Temperature Deposition of XRD-Amorphous TiO2 Thin Films: Investigation of Device Performance as a Function of Temperature. *Ceram. Int.* **2018**, *44*, 11582–11590. [CrossRef]
276. D'Elia, A.; Cibin, G.; Robbins, P.E.; Maggi, V.; Marcelli, A. Design and Characterization of a Mapping Device Optimized to Collect XRD Patterns from Highly Inhomogeneous and Low Density Powder Samples. *Nucl. Instrum. Methods Phys. Res. Sect. B Beam Interact. Mater. Atoms* **2017**, *411*, 22–28. [CrossRef]
277. Bunaciu, A.A.; Udriştioiu, E.G.; Aboul-Enein, H.Y. X-ray Diffraction: Instrumentation and Applications. *Crit. Rev. Anal. Chem.* **2015**, *45*, 289–299. [CrossRef] [PubMed]

278. Ameh, E.S. A Review of Basic Crystallography and X-ray Diffraction Applications. *Int. J. Adv. Manuf. Technol.* **2019**, *105*, 3289–3302. [CrossRef]
279. Li, Y.; Wu, S.; Amirkhanian, S. Investigation of the Graphene Oxide and Asphalt Interaction and Its Effect on Asphalt Pavement Performance. *Constr. Build. Mater.* **2018**, *165*, 572–584. [CrossRef]
280. Ali, A.; Chiang, Y.W.; Santos, R.M. X-ray Diffraction Techniques for Mineral Characterization: A Review for Engineers of the Fundamentals, Applications, and Research Directions. *Minerals* **2022**, *12*, 205. [CrossRef]
281. Holder, C.F.; Schaak, R.E. Tutorial on Powder X-ray Diffraction for Characterizing Nanoscale Materials. *ACS Nano* **2019**, *13*, 7359–7365. [CrossRef]
282. Zhang, X.-L.; Guo, Y.-D.; Su, J.-F.; Han, S.; Wang, Y.-Y.; Tan, Y.-Q. Investigating the Electrothermal Self-Healing Bituminous Composite Material Using Microcapsules Containing Rejuvenator with Graphene/Organic Hybrid Structure Shells. *Constr. Build. Mater.* **2018**, *187*, 1158–1176. [CrossRef]
283. Guo, S.; Dai, Q.; Wang, Z.; Yao, H. Rapid Microwave Irradiation Synthesis of Carbon Nanotubes on Graphite Surface and Its Application on Asphalt Reinforcement. *Compos. Part B Eng.* **2017**, *124*, 134–143. [CrossRef]
284. Le, J.; Marasteanu, M.; Turos, M. Graphene Nanoplatelet (GNP) Reinforced Asphalt Mixtures: A Novel Multifunctional Pavement Material. *Final Rep. NCHRP IDEA Proj.* **2016**, *173*, 1–29.
285. Rousso, I.; Deshpande, A. Applications of Atomic Force Microscopy in HIV-1 Research. *Viruses* **2022**, *14*, 648. [CrossRef] [PubMed]
286. Lee, K.; Kim, S. Performance Improvement Effect of Asphalt Binder Using Pyrolysis Carbon Black. *Materials* **2022**, *15*, 4158. [CrossRef] [PubMed]
287. Fadley, C.S. X-ray Photoelectron Spectroscopy: Progress and Perspectives. *J. Electron Spectros. Relat. Phenomena* **2010**, *178–179*, 2–32. [CrossRef]
288. Giechaskiel, B.; Clairotte, M. Fourier Transform Infrared (FTIR) Spectroscopy for Measurements of Vehicle Exhaust Emissions: A Review. *Appl. Sci.* **2021**, *11*, 7416. [CrossRef]
289. Tu, Q.; Chang, C. Diagnostic Applications of Raman Spectroscopy. *Nanomed. Nanotechnol. Biol. Med.* **2012**, *8*, 545–558. [CrossRef]
290. Mariano, R.G.; Yau, A.; McKeown, J.T.; Kumar, M.; Kanan, M.W. Comparing Scanning Electron Microscope and Transmission Electron Microscope Grain Mapping Techniques Applied to Well- Defined and Highly Irregular Nanoparticles. *ACS Omega* **2020**, *5*, 2791–2799. [CrossRef]
291. Le Parlouër, P. Chapter 2: Thermal Analysis and Calorimetry Techniques for Catalytic Investigations. *Springer Ser. Mater. Sci.* **2013**, *154*, 51–101. [CrossRef]
292. Gumustas, M.; Sengel-Turk, C.T.; Gumustas, A.; Ozkan, S.A.; Uslu, B. Chapter 5: Effect of Polymer-Based Nanoparticles on the Assay of Antimicrobial Drug Delivery Systems. In *Multifunctional Systems for Combined Delivery, Biosensing and Diagnostics*; Elsevier: Amsterdam, The Netherlands, 2017; pp. 67–108. [CrossRef]
293. Nandhakumar, M.; Thangadurai, D.T.; Kasi, N. Topical Progress of Gold Nanoparticles towards Diverse Metal Ion Sensing through Optical Spectrometry and Electrochemical Techniques—A Short Review. *J. Mater. Res. Technol.* **2022**, *22*, 1185–1209. [CrossRef]
294. Zhang, B.; Gu, B.; Tian, G.; Zhou, J.; Huang, J.; Xiong, Y. Challenges and Solutions of Optical-Based Nondestructive Quality Inspection for Robotic Fruit and Vegetable Grading Systems: A Technical Review. *Trends Food Sci. Technol.* **2018**, *81*, 213–231. [CrossRef]
295. Kumar, S.; Himanshi; Prakash, J.; Verma, A.; Suman; Jasrotia, R.; Kandwal, A.; Verma, R.; Godara, S.K.; Khan, M.A.M.; et al. A Review on Properties and Environmental Applications of Graphene and Its Derivative-Based Composites. *Catalysts* **2023**, *13*, 111. [CrossRef]
296. Li, S.; Luo, H.; Hu, M.; Zhang, M.; Feng, J.; Liu, Y.; Dong, Q.; Liu, B. Optical Non-Destructive Techniques for Small Berry Fruits: A Review. *Artif. Intell. Agric.* **2019**, *2*, 85–98. [CrossRef]
297. Liu, S.; Guo, C.; Sheridan, J.T. A Review of Optical Image Encryption Techniques. *Opt. Laser Technol.* **2014**, *57*, 327–342. [CrossRef]
298. Kulkarni, S.C.; Rege, P.P. Pixel Level Fusion Techniques for SAR and Optical Images: A Review. *Inf. Fusion* **2020**, *59*, 13–29. [CrossRef]
299. Bruno, L. Mechanical Characterization of Composite Materials by Optical Techniques: A Review. *Opt. Lasers Eng.* **2018**, *104*, 192–203. [CrossRef]
300. Wang, Y.; Xie, F.; Ma, S.; Dong, L. Review of Surface Profile Measurement Techniques Based on Optical Interferometry. *Opt. Lasers Eng.* **2017**, *93*, 164–170. [CrossRef]
301. Devi, P.; Jain, R.; Thakur, A.; Kumar, M.; Labhsetwar, N.K.; Nayak, M.; Kumar, P. A Systematic Review and Meta-Analysis of Voltammetric and Optical Techniques for Inorganic Selenium Determination in Water. *Trends Anal. Chem.* **2017**, *95*, 69–85. [CrossRef]
302. Linne, M. Imaging in the Optically Dense Regions of a Spray: A Review of Developing Techniques. *Prog. Energy Combust. Sci.* **2013**, *39*, 403–440. [CrossRef]
303. Jiao, F.; Liu, L.; Cheng, W.; Li, C.; Zhang, X. Review of Optical Measurement Techniques for Measuring Three-Dimensional Topography of Inner-Wall-Shaped Parts. *Measurement* **2022**, *202*, 111794. [CrossRef]
304. Li, L.; Chen, S.; Deng, M.; Gao, Z. Optical Techniques in Non-Destructive Detection of Wheat Quality: A Review. *Grain Oil Sci. Technol.* **2022**, *5*, 44–57. [CrossRef]

305. Abdlaty, R.; Hayward, J.; Farrell, T.; Fang, Q. Skin Erythema and Pigmentation: A Review of Optical Assessment Techniques. *Photodiagnosis Photodyn. Ther.* **2021**, *33*, 102127. [CrossRef]
306. Khan, S.; Le Calvé, S.; Newport, D. A Review of Optical Interferometry Techniques for VOC Detection. *Sens. Actuators A Phys.* **2020**, *302*, 111782. [CrossRef]
307. Islam, S.; Sufian, A.; Hossain, M.; Miller, R.; Leibrock, C. Mechanistic-Empirical Design of Perpetual Pavement. *Road Mater. Pavement Des.* **2020**, *21*, 1224–1237. [CrossRef]
308. Lee, S.I.; Carrasco, G.; Mahmoud, E.; Walubita, L.F. Alternative Structure and Material Designs for Cost-Effective Perpetual Pavements in Texas. *J. Transp. Eng. Part B Pavements* **2020**, *146*, 04020071. [CrossRef]
309. Kulkarni, S.; Ranadive, M.S. The Parametric Comparison of Perpetual Pavements with Respect to Life-Cycle Cost and Greenhouse Gas Emissions. *Mater. Today Proc.* **2022**, *52*, 1147–1152. [CrossRef]
310. Walubita, L.F.; Scullion, T.; Leidy, J.; Liu, W. Non-Destructive Testing Technologies: Application of the Ground Penetrating Radar (GPR) to Perpetual Pavements. *Road Mater. Pavement Des.* **2009**, *10*, 259–286. [CrossRef]
311. Xie, Z.; Shen, J. Effect of Weathering on Rubberized Porous European Mixture. *J. Mater. Civ. Eng.* **2016**, *28*, 04016043. [CrossRef]